

Vision-Enhanced Communications: On the Benefits of NLOS/LOS Knowledge in Wireless Systems

Samuel B. Brown

Thesis submitted to the Faculty of the
Virginia Polytechnic Institute and State University
in partial fulfillment of the requirements for the degree of

Master of Science
in
Electrical Engineering

Harpreet S. Dhillon, Chair

Richard M. Buehrer

William C. Headley

May 5, 2025

Blacksburg, Virginia

Keywords: Sensors, Internet of Things, LOS/NLOS, Out-of-Band Knowledge, CFAR, CTMC,
Markov Channel, Dynamic Channel, Composite Hypothesis Testing

Copyright 2025, Samuel B. Brown

Vision-Enhanced Communications: On the Benefits of NLOS/LOS Knowledge in Wireless Systems

Samuel B. Brown

(ABSTRACT)

The proliferation of Internet of Things (IoT) devices equipped with meteorological, auditory, optical, and infrared sensors has opened the door to integrating sensor-based information into existing physical layer communication system design. Many properties of the wireless channel, especially for mobile applications, are highly dynamic and easily observable using non-radio frequency (RF) sensors or RF sensors operating out-of-band (OOB) which we refer to as *vision sensors*. Using vision sensors to provide information about one such property, that of line-of-sight (LOS)/non-line-of-sight (NLOS) states, is the central focus of this work. A generalized signal detection framework is presented for a vision sensor-aided receiver operating in a binary continuous-time Markov chain (CTMC) channel environment wherein the NLOS/LOS state toggles intermittently. Several cases are explored wherein varying degrees of NLOS/LOS knowledge are available at the receiver with an emphasis on labeled vs unlabeled information. Bayes risk and composite likelihood ratio test (LRT) methods are used to derive the optimal decision rule in both constant false-alarm rate (CFAR) and minimum probability of error ($\min(P_e)$) paradigms. It is shown that a dynamic detection scheme utilizing labeled information, including imperfect error-prone labels, sourced from vision sensors can improve upon the uniformly-most-powerful (UMP) test in an ensemble of trials, yielding higher CFAR detection rates than static detectors without vision sensors. Further, it is shown that unlabeled information, while matching the CFAR performance of the UMP test, can yield a lower overall error rate compared to a *blind* receiver with no NLOS/LOS knowledge.

Vision-Enhanced Communications: On the Benefits of NLOS/LOS Knowledge in Wireless Systems

Samuel B. Brown

(GENERAL AUDIENCE ABSTRACT)

The proliferation of Internet of Things (IoT) devices equipped with meteorological, auditory, optical, and infrared sensors has opened the door to integrating sensor-based information into existing wireless communication system design. Many properties of the radio frequency (RF) channel, especially for mobile applications, are highly dynamic and easily observable using sensors operating out-of-band (OOB) such as optical and infrared (IR) cameras and radars operating in different frequency ranges. These *vision sensors* can provide information about the physical propagation environment beyond what is typically sensed with an existing RF receiver. This work explores the benefits of using vision sensors to determine whether a communication link is line-of-sight (LOS) with a direct path to the transmitter or non-line-of-sight (NLOS) without a direct path. A performance analysis is presented for a receiver with vision information using classical hypothesis testing and detection theory, and a generalized framework is presented to compare performance with perfect vision information and imperfect error-prone information. It is shown that using a dynamic detector, which can adjust its sensitivity based on information about the NLOS/LOS state, can improve its detection performance over a static detector which lacks vision information. This result demonstrates that wireless communications systems can indeed benefit from vision sensors, even if the information they provide is partially corrupted and not always available.

Dedication

To my parents Mike and Bonnie and my sister Eliana.

Acknowledgments

I would like to lend here my sincere thanks to all who have mentored, inspired, taught, and entertained me over the past two years during my graduate studies and during my undergraduate years as well. This crazy journey I've undertaken called graduate school has taught me how to think about things that have not yet been thought about, and for that I owe enormous gratitude to many individuals.

I first met my advisor, Dr. Harpreet Dhillon, while taking *Introduction to Communications Systems* in my junior year of undergrad. This was in fact the course that drove me to study wireless, and I knew very quickly Dr. Dhillon would make a good advisor because of his knack for boiling down complex concepts into digestible pieces. I started working with him the following year, and he proved essential to guiding me towards the research mindset- that is- moving away from the solving-problems-given-to-you mindset and towards the solving-novel-problems one. I didn't realize how valuable this transition was at the time, but looking back now I do. I also took his *Stochastic Signals and Systems* course later which proved to be essential to my work and helped solidify my understanding of everything else in the field.

I would also like to thank some other teachers that have helped lead me to where I am. Dr. R. Michael Buehrer's course on *Multi-Channel Communications* proved to be another invaluable, solidifying experience which brought much of the mystifying world of the physical layer into focus for me. Additionally Dr. Alan Michaels' *Spread Spectrum Communications* and Dr. Scotland Lemans' courses on *Bayesian Statistics* and *Statistical Inference* were indispensable.

I would be foolish not to mention the support of some other mentors of mine. I am privileged to have worked with Dr. Charlie Thornton and Dr. William (Chris) Headley during my time at NSI/Hume, both of whom were excellent partners throughout my RF Machine Learning work and helped me hone my presentation skills.

And now I must extend my appreciation to those colleagues who made everything easier through

moral support and entertainment. Samantha Frietchen for being an excellent partner-in-crime throughout so so many courses, Nick Goradia for being a good research partner and roommate all-in-one, Gaurav Duggal for being the best wireless biking club lead and most likely to illegally transmit in our group (except me), Tom Anders for being an excellent radio turbine partner, Anish Pradhan for great research advice and entertainment, and to Harish Dureppagari, Haozhou Hu, Xiangliu Tu, Don-Roberts Emenonye, and Wasif Hussain for being great lab-mates.

Lastly I would like to thank my family including my cousin Marc Lichtman, my mom, Bonnie Brown, my dad, Mike Brown, and my sister Eliana Brown for their unending support.

Contents

List of Figures	ix
1 Background	1
1.1 Taxonomy of Vision Information	2
1.2 Problem Formulation	6
1.3 Published Works	9
2 Improving Receiver Detection Performance Through NLOS/LOS Vision	10
2.1 Introduction	10
2.2 System Model	12
2.2.1 Cases Involving Varying Levels of Knowledge	14
2.3 Detection Framework	15
2.3.1 M -ary Detection using Bayes Risk	16
2.3.2 Binary Composite Hypothesis Testing	19
2.3.3 Performance Analysis	21
2.4 Case-Based Analysis	25
2.4.1 Labeled Knowledge (Vision)	25
2.4.2 Statistical Knowledge	25

2.4.3	Blind	26
2.5	Numerical Results and Discussion	28
2.6	Conclusions and Future Work	29
3	Optimal Performance of Vision Sensor-Aided Receivers with Imperfect Information	31
3.1	Introduction	31
3.1.1	Prior Work	33
3.1.2	Contributions and Problem Setup	35
3.2	System Model	36
3.2.1	Knowledge at the Receiver	40
3.3	Generalized Detection Framework	42
3.3.1	Generalized Detection Performance	47
3.4	Optimal Detection with Periodic Labels	52
3.4.1	Performance Analysis with Periodic Labels	57
3.5	Numerical Results and Discussion	60
4	Conclusion	65
	Bibliography	67

List of Figures

1.1	Taxonomy of Vision Information	3
2.1	Received signal amplitude over time.	12
2.2	Channel model.	14
2.3	Piecewise-linear approximation vs exact detector.	21
2.4	ROC curve (CFAR) performance: vision vs UMP test.	28
2.5	Prob. of error performance: vision vs statistical vs blind	29
3.1	CTMC channel and label processes over time	38
3.2	Optimal decision statistic with upper and lower bounds	46
3.3	LOS prob. estimate $\hat{q}(t)$ at the receiver with CTMC channel state $\Psi(t)$ and CTMC rates of $\lambda' = \{0.5, 0.1, 0.01\}$	56
3.4	Simulated and calculated ROC curves for Perfect Vision (PV), Periodic Labels (PL), and UMP test with $\text{SNR}_{avg} = 8$ dB, $q = \{0.2, 0.5, 0.8\}$, $\alpha_2/\alpha_1 = 10$, $\lambda' = 0.1$, $\tau_L = 1$	61
3.5	CFAR Prob. of Detection vs avg. SNR for Perfect Vision (PV), Periodic Labels (PL), and UMP test with Target $P_{FA} = 0.1$, $q = 0.7$, $\alpha_2/\alpha_1 = 10$, $\lambda' = 0.1$, $\tau_L = 1$	62

3.6	CFAR Prob. of Detection vs label period (τ_L) for Perfect Vision (PV), Periodic Labels (PL), and UMP test with Target $P_{FA} = 0.1$, $q = 0.7$, $\alpha_2/\alpha_1 = 10$, $\lambda' = 0.1$, $\epsilon = \{0, 0.1, 0.2\}$	63
3.7	Probability of Error vs avg. SNR for Perfect Vision (PV), Periodic Labels (PL), Statistical (S), and Blind (B) with $q = 0.9$, $\alpha_2/\alpha_1 = 100$, $\lambda' = 0.1$, $\epsilon = 0.1$, $\tau_L = 1$	64

List of Abbreviations

P_D Probability of Detection

P_{FA} Probability of False-Alarm

AI Artificial Intelligence

AWGN Additive White Gaussian Noise

CFAR Constant False-Alarm Rate

CTMC Continuous Time Markov Chain

GLRT Generalized Likelihood Ratio Test

IID Independent and Identically Distributed

IoT Internet of Things

LOS Line-of-Sight

LRT Likelihood Ratio Test

MAP Maximum a Posteriori

mMIMO Massive Multiple-Input-Multiple-Output

NLOS Non-Line-of-Sight

OOK On-Off Keying

RF Radio Frequency

SNR Signal to Noise Ratio

SOI Signal of Interest

UMP Uniformly Most Powerful

Chapter 1

Background

Sensors surround us in nearly every aspect of our lives. The cameras, microphones, antennas, thermometers, barometers, accelerometers, hygrometers, and magnetometers that accompany us in our pockets, in our homes and in our cars are the sources of much of the seemingly endless digital information generated by human activities each day, a whopping 500 Terabytes of data [2]. Sensors of all kinds are estimated to account for around 44% of this [3]. The ubiquity of sensors can largely be attributed to our increasing desire to connect ourselves to the rest of the world by way of the internet, necessitating carrying cameras and microphones in our pockets wherever we go. Another significant driver of our sensor-filled world is the rise of automation and artificial intelligence (AI) which have an insatiable appetite for sensor data, only projected to grow in the coming years.

In addition to carrying the sensors around in our pockets, they enable many of the *things* running in the background of our civilization like street lights, utility meters, and water mains to communicate with everything else. It is the integration of machines and global communication and machine-to-machine (M2M) communication that necessitates the internet of things (IoT). The increasing use of IoT in wide-area networks and mobile applications leaves plenty of room for innovation for sixth-generation cellular standards (6G) and non-terrestrial network (NTN) standards [4].

This work is concerned with the interconnection of these sensors and the ways in which their presence in our lives overlaps with the wireless communications infrastructure required for

their data to infiltrate the world-wide-web. Wherever IoT and sensors are needed, there is a corresponding need for communication infrastructure, which in many cases predates the need for IoT. Cellular networks, for instance, have existed in some shape or form since the early 1980s for the purposes of human voice communications. Only in the past 20 years, however, have these networks begun to incorporate IoT devices. Fortunately, the relatively low data rates required by most IoT devices mean that adequate room within the channel capacity can usually be allocated beyond that used by mobile hand-held devices.

Although individual IoT devices can often operate without the need for high data-rates, accommodating the number of IoT network users within a given area can account for a significant chunk of radio resources. This work examines the value in using IoT sensors to aid existing wireless systems rather than being solely consumers of physical layer resources.

1.1 Taxonomy of Vision Information

The dynamic physical environments in which many modern wireless applications operate such as vehicle-to-everything communication, next-generation cellular, unmanned aerial vehicle (UAV) communication, and indoor positioning technology are becoming increasingly reliant upon millimeter wave (mmWave) frequencies, with terahertz (THz) frequencies on the horizon. Due to the propensity for electromagnetic radiation in this regime to behave more like optical frequencies than radio frequencies, the geometry of the channel environment plays a more direct role in propagation behavior [5]. Geometric information such as the existence of a line-of-sight (LOS) path, angles of arrival and departure, the placement of indirect paths, and the placement of reflectors, although affecting the propagation behavior of any radio frequency band, have a better-defined effect on shorter wavelength bands such as mmWave and THz.

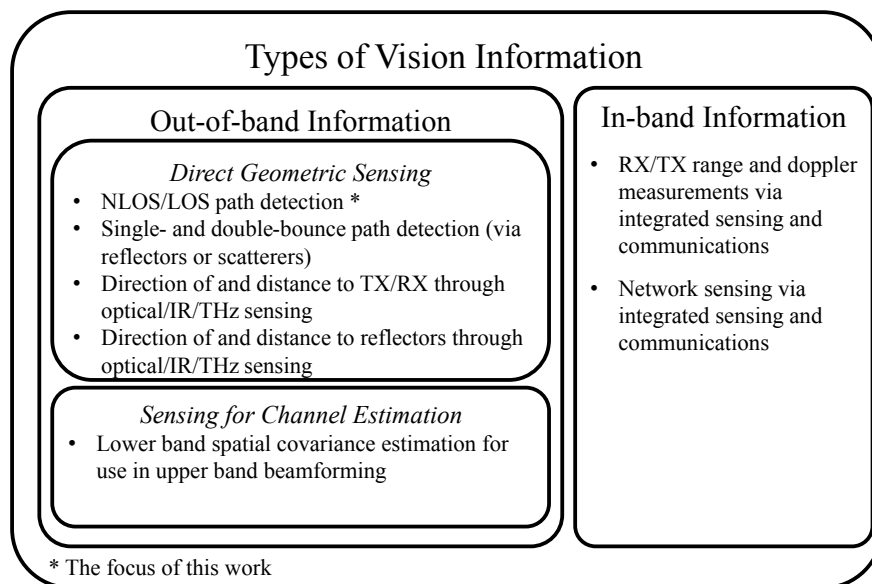


Figure 1.1: Taxonomy of Vision Information

Vision sensors, which are often optical or infrared (IR), provide an opportunity to gather geometric information about the channel environment directly which is often more efficient in terms of overhead than obtaining this information in-band using the existing radio frequency (RF) hardware. There are numerous types of geometric information which can be gathered, some providing more useful information than others to the performance of the accompanying physical layer communications or radar system.

One can gain a better understanding of the relevance of this work if one is familiar with the broader landscape within which it resides. To this end, we delve into the types of vision information one can obtain, discuss their usage in the literature, and discuss how vision sensors might be able to enhance performance by providing this information. The broad classification of vision-enhanced communications can be thought of as communications with the addition of out-of-band information. This can encompass any information about the channel provided to the transmitter or the receiver beyond that which the existing RF system can obtain. Traditional channel estimation, for instance, would not be an example of

vision information because it utilizes the existing RF band to sample the channel. Performing channel estimation at lower frequencies to provide spatial covariance information for a higher frequency communication link, however, would indeed be an example of vision.

To classify types of vision information, we start first with the distinction between in-band and out-of-band information. This property is based purely on the frequency band within which the sensor operates and whether that band overlaps with the RF band used for the actual communication or radar function of the system. Unsurprisingly, out-of-band sensors make up the vast majority with optical, IR, LiDAR, and simply higher or lower frequency RF sensors all comprising out-of-band sensing. In-band sensing is primarily relevant in the realm of integrated sensing and communications (ISAC) which has been thoroughly explored in the literature. ISAC systems are designed specifically to enable the dual use of the RF hardware at the transmitter or receiver by combining sensing functionality in the form of radar with communications functionality [6]. Although such techniques can be considered vision-enhanced wireless, their benefits differ from out-of-band techniques.

In-band sensing has appeared most prominently in communication-centric ISAC because the sensor, in most cases a radar system, is treated as an enhancement to an existing communications system. Such an arrangement can exploit geometric transformations between channel parameters such as the user's position and orientation along with providing networking sensing information involving range and Doppler measurements of targets and reflectors which happen to be users of the communication system [6]. The concept of using in-band RF sensors to obtain spatial and physical parameters in the channel environment has been referred to as a *perceptive network* [7, 8]. These networks combine sensing capabilities with existing communications functionality including urban traffic monitoring, weather observation, and human activity recognition, not all of which are useful for enhancing physical layer performance. For this reason, the in-band vision sensing which is of interest to this work is only

a subset of perceptive network capabilities. Within this subset, [9] provides an example of vision sensing for ISAC which is shown to be beneficial from an information theoretic perspective.

Out-of-band vision encompasses a large array of techniques and is most relevant to this work. These sensors which provide information beyond what the existing RF hardware can provide can be separated into two primary groups: *direct geometric sensing* and *sensing for channel estimation*. The former refers to the gathering of certain geometric properties of the channel environment often used to parameterize some geometric channel model. The latter refers to the use of out-of-band RF sensors for channel estimation in the more traditional multiple-input-multiple-output (MIMO) sense.

Direct geometric sensing is most relevant when dealing with specific geometric channel models such as those used for UAVs and other high-mobility environments in conjunction with mmWave and THz. [10] provides an example of such a model wherein the received signal is a superposition of the LOS component and single-bounce rays from scatterers whose positions are stochastic in nature. The THz channel model presented in [11] utilizes a 3D ray-launching algorithm which characterizes absorption and scattering properties of different materials. The role of direct geometric sensing in these sorts of models is to fill in gaps of information regarding the existence of the LOS path, the existence of scatterer paths, location and velocity of the TX/RX, location and velocity of scatterers, and types of materials in the environment, all of which are far easier to ascertain in the optical and IR domains rather than RF.

The other category of out-of-band sensing, sensing for channel estimation, performs tasks more reminiscent of traditional in-band channel estimation, which itself is not a form of vision. However, if an RF system performs channel estimation out-of-band, typically at lower frequencies, this qualifies as vision-enhanced wireless. The most prominent examples

of this occur in mMIMO mmWave systems wherein link configuration and beam training at the high frequencies used for operation presents a significant source of overhead. One can therefore enhance the beamforming performance in the desired band of operation by using a sub-6GHz antenna array to estimate channel parameters such as the spatial covariance [12]. Architectures which utilize such out-of-band channel estimation are also beneficial when dealing with the hardware constraints in the mmWave and THz bands. Such high frequency arrays typically use either all-analog or a hybrid analog-digital beamforming architecture wherein full spatial covariance estimation is not possible. Sub-6GHz arrays, however, can be made fully digital more easily, enabling full covariance estimation out-of-band. The spatial information gathered at the lower frequencies can then be used for precoding in the desired band of operation [13].

1.2 Problem Formulation

Having explored the broader landscape of vision information establishing the context for this work, the crux of the upcoming analysis can be discussed. Within the taxonomy described the most relevant type of vision information to this work is that of LOS path detection, a form of direct geometric sensing, in turn a form of out-of-band information. Out of all forms of geometric information one can obtain about the channel environment, the existence of a LOS path is arguably the simplest. Its binary nature and direct impact on the SNR at the receiver lend themselves well to a fundamental detection theoretic analysis, and expansion to more complex geometric parameters such as the direction of arrival of scattered signals is entirely possible.

The foundation of this work is a seemingly simple detection problem in which a transmitter and receiver experience either LOS or NLOS conditions with some probability. The receiver

must detect the presence of some DC signal in additive white Gaussian noise (AWGN) while optionally possessing some labels regarding the LOS state. The seemingly trivial nature of this problem stems from its striking similarity to the classic problem involving the detection of a DC signal in AWGN. Working through the scenario carefully, however, reveals a surprisingly nuanced problem involving multiple cases of knowledge with varying fidelity and availability.

The original analysis involves the use of the Neyman Pearson detector with a modification allowing for three rather than two hypotheses. The likelihood ratio test (LRT) $\frac{p(x; \mathcal{H}_1)}{p(x; \mathcal{H}_0)} > \gamma$ is the logical choice for a binary detector, but a different approach must be used for the NLOS/LOS problem because it is not a simple binary hypothesis problem [14, p.94-105]. Taking into account the NLOS/LOS state, there are in fact three hypotheses at the receiver: $\mathcal{H}_0 \sim$ no-signal, $\mathcal{H}_1 \sim$ signal with NLOS, and $\mathcal{H}_2 \sim$ signal with LOS. This realization leads to treating the problem as an *M-ary* hypothesis testing problem wherein, unlike the traditional Neyman Pearson Lemma, a Bayesian approach with prior knowledge is required [14, p.119-125].

Further developing the problem analysis, an important distinction between constant-false-alarm-rate (CFAR) hypothesis testing and minimum probability of error ($\min(P_e)$) hypothesis testing arises. The Neyman Pearson Lemma and LRT define a test purely based on the ratio between the likelihoods of two possible outcomes. *M-ary* detection, however, cannot be defined as a ratio and therefore requires weights for the likelihoods. The Bayesian approach provides exactly what is needed here by introducing prior probabilities as weights. The derivation of the *M-ary* test, however, involves minimizing the total probability of error involving both Type-I and Type-II errors, whereas the LRT relies on choosing an arbitrary detection threshold base upon Type-I errors only.

Treating the problem as a *3-ary* hypothesis testing problem introduces an important knob

to manipulate: the knowledge of the NLOS/LOS state. Fully incorporating this knowledge into the detection analysis, however, requires treating the problem in a slightly different way. Rather than considering three hypotheses with deterministic signals for each, one can consider only two but with an unknown parameter. Here, the technique of composite hypothesis testing becomes incredibly useful, allowing one to derive optimal detection rules wherein some unknown parameter exists within the signal. As the NLOS/LOS state translates directly to received signal strength, it is only logical that this unknown parameter be the received signal amplitude, A_s . Various techniques exist for this variety of detection problem include the generalized likelihood ratio test (GLRT), Rao, and Wald tests, but it is the Bayesian which allows full treatment of the distribution of this unknown parameter [14, p.253-260].

One of the greatest sources of nuance in the NLOS/LOS problem emerges from the treatment of the types of knowledge the receiver obtains about the NLOS/LOS state. Questions arise such as: Does the receiver obtain labels about the LOS state or simply knowledge of its probability? What happens when no knowledge whatsoever is available regarding LOS? What happens when the labels are imperfect and subject to error? The composite hypothesis testing approach provides an avenue through which to consider all of these questions by incorporating the distribution of the known parameter, the received signal amplitude, for each case of knowledge.

The aim of this work is to spell out the gains one may achieve by piping information about the existence of the LOS path to a receiver using classical detection and estimation theory. The nature of the vision sensors themselves, however, are not relevant to this work, but information sourced from realistic sensors can be analyzed using the framework presented here.

Chapter 2 provides a succinct, but careful analysis of three basic cases of NLOS/LOS knowl-

edge and presents the optimal detection rules at the receiver for each case. CFAR and $\min(P_e)$ performance is presented there for each case with comparisons made. Chapter 3 provides a more comprehensive treatment of the problem by emphasizing the continuous-time behavior of an intermittent NLOS/LOS channel environment. There a framework is presented which takes into account the imperfections of real vision sensors, and the enhancements that can be made to detection performance are shown through this lens.

1.3 Published Works

Related to this thesis:

- S. B. Brown and H. S. Dhillon, “Improving Receiver Detection Performance Through NLOS/LOS Vision,” *MILCOM 2024 - 2024 IEEE Military Communications Conference (MILCOM)*, Washington, DC, USA, 2024, pp. 1-6.
- Journal Submission: S. B. Brown and H. S. Dhillon, “Optimal Performance of Vision-Aided Receivers with Imperfect Information,” May 2025.

Others:

- S. B. Brown et al., “Aircraft Radar Altimeter Interference Mitigation Through a CNN-Layer Only Denoising Autoencoder Architecture,” *MILCOM 2024 - 2024 IEEE Military Communications Conference (MILCOM)*, Washington, DC, USA, 2024, pp. 306-311.
- S. Brown, G. Niculescu, and I. Niculescu, “Machine learning representation of the F2 structure function over all charted Q2 and x range,” *Phys. Rev. C*, vol. 104, p. 064321, Dec 2021.

Chapter 2

Improving Receiver Detection

Performance Through NLOS/LOS

Vision

2.1 Introduction

In modern communications systems there are often numerous opportunities to obtain external knowledge about the channel beyond that which is provided by the receiver itself, such as knowledge obtained through optical and radio frequency (RF) sensors operating outside of the main system frequency band; e.g., radar systems aided by optical sensors or cellular base stations aided by LOS infra-red sensors. Sensors of all varieties are abundant in the mobile devices we use and crucial to the functionality of wireless IoT devices, smart vehicles, and satellites. In this paper we explore the benefits that can be garnered from this external knowledge or “vision” through the lens of detection theory and hypothesis testing and apply these tools to a dynamic communications channel.

Arguably the simplest of classical signal detection problems is that of the constant DC value in additive white Gaussian noise (AWGN). The problem explored in this work generalizes this to arbitrary pulse shapes and introduces a stochastic element into the channel behavior while

accounting for varying levels of information provided by the vision sensor. As with numerous other practical detection scenarios without fully-known distributions for each hypothesis, there are unknown parameters that must be accounted for when obtaining the optimal decision rule. Two approaches which address the unknown parameter detection problem from different angles are outlined in the literature; namely, the m -ary hypothesis approach and the composite hypothesis approach [14]. The latter is further broken down into the generalized likelihood ratio test (GLRT), Rao, and Wald tests which are asymptotically optimal for MLE estimates of the unknown parameter(s) with independent and identically-distributed (IID) data [15, 16, 17]. The GLRT, Rao, and Wald tests, however, do not take into account prior knowledge of the distribution of the parameter itself whereas the Bayesian composite hypothesis testing method does [18, 19, 20]. As this prior distribution is known in the problem at hand, it should logically be factored into the detection scheme.

Here we present an analysis of one such detection problem involving an unknown parameter whose state can be optionally obtained through a label. The parameter in question represents a Bernoulli channel state of either line-of-sight (LOS) or non-line-of-sight (NLOS), much like the characterization used in [21]. [22] provides another application in which a mixed NLOS/-LOS environment is considered. The legitimacy of the uniformly-most-powerful (UMP) test is challenged for cases where the test statistic does not depend on the unknown parameter [23]. In the scenario presented, even though a UMP test does exist in a constant-false-alarm-rate (CFAR) detection paradigm, it is shown that, by adopting a dynamic detection scheme, one can achieve a higher probability of detection over an ensemble of trials for a given false alarm rate than that achieved through the UMP test. Further, given prior probabilities for the hypotheses, one can achieve a lower probability of error given knowledge of the parameter distribution than without.

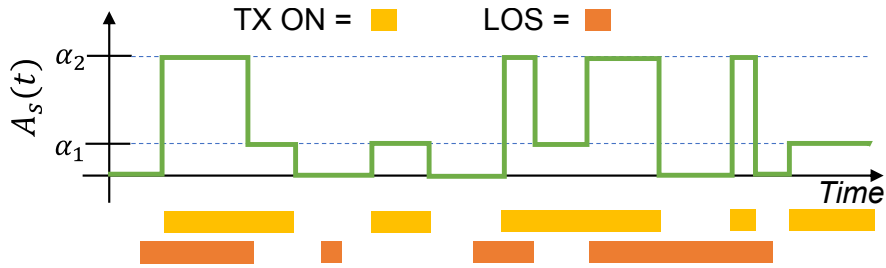


Figure 2.1: Received signal amplitude over time.

2.2 System Model

We construct a simple detection scenario in which a receiver must determine the presence of a signal with known pulse shape in an AWGN channel. The amplitude of the received signal, however, is random and depends upon the channel state which can either be LOS or NLOS. Specifically, the channel state Ψ can take on one of two possible values: $\Psi(t) \in \{\text{NLOS}, \text{LOS}\}$. This provides a simple model for a dynamic wireless link which toggles intermittently between NLOS and LOS such that the state Ψ is a correlated Bernoulli random variable as in [21]. For the sake of the problem at hand, we will assume $\Psi(t)$ is governed by a Markov switching random process, also known as a continuous time Markov chain (CTMC).

$$\begin{aligned} \Psi(t) | \{t = t_0\} &\sim \text{Bernoulli}(q) \\ P(\Psi(t) | \{t = t_0\}) &= \left\{ \begin{array}{ll} 1 - q, & \Psi = 0 \text{ (NLOS)} \\ q, & \Psi = 1 \text{ (LOS)} \end{array} \right\} \end{aligned} \quad (2.1)$$

The marginal distribution of $\Psi(t)$ is shown in (2.1). Our model establishes α_1 and α_2 as the amplitudes the received signal will assume in the NLOS and LOS states, respectively, with condition $\alpha_2 > \alpha_1$. Additionally, the signal is assumed to be present at times and absent at other times as in an on-off-keying (OOK) scenario for communications or a target in range/Doppler space for radar. This means that the received signal amplitude

can take on three distinct values $A_s(t) \in \{0, \alpha_1, \alpha_2\}$ representing the no-signal, NLOS, and LOS cases. Figure 2.1 illustrates the behavior of the received signal amplitude $A_s(t)$ as a function of time in the midst of the intermittent channel state $\Psi(t)$ (shown in orange) and the OOK behavior at the transmitter (shown in yellow). One can notice how the channel state and signal state appear independent of one another, and indeed we assume that $A_s(t)$ and $\Psi(t)$ follow two independent random processes. The received signal has shape $P(t)$, and we assume that this shape is known at the receiver and that time alignment has been achieved; i.e. coherent reception is possible. The form of the received signal without noise is therefore $s(t) = A_s(t)P(t)$. The true received signal is corrupted in the channel by a white noise process $n(t)$ which is added to the received signal $s(t)$. The observation made by the receiver is then a vector of N samples, $\vec{r}(k)$, and we assume that the channel state $\Psi(t)$ does not change over the duration of the observation; i.e. the amplitude value $A_s(t)$ remains constant for the entire vector $\vec{r}(k)$, taking on a single value which we denote A_s . The decision regarding the presence of the signal is then made based upon the information obtained in $\vec{r}(k)$. The marginal probability distributions for a single noise sample n_k and a single signal sample s_k are shown in (2.2) for which σ_n^2 is the noise variance, P_k is a sample from the known signal shape, π_0 is the prior probability of the no-signal (only noise) state ($1 - Pr[A_s = 0]$), and q is the probability of LOS ($Pr[\Psi(t) = 1 | \{t = t_k\}]$).

$$\vec{r}(k) = \vec{n}(k) + \vec{s}(k) = \vec{n}(k) + A_s \vec{P}(k),$$

where

$$n_k \sim \mathcal{N}(0, \sigma_n^2), \tag{2.2}$$

$$\text{and } s_k \sim f_{s_k}(s) = \begin{cases} \pi_0, & s = 0 \\ (1 - \pi_0)(1 - q), & s = \alpha_1 P_k \\ (1 - \pi_0)q, & s = \alpha_2 P_k \end{cases}$$

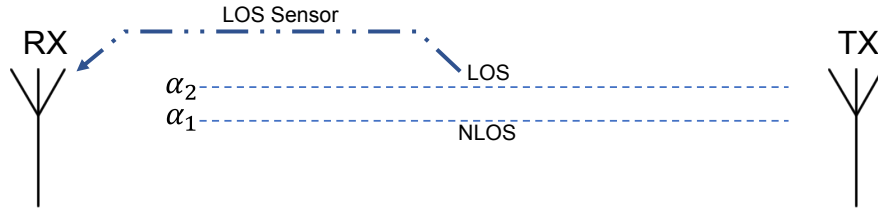


Figure 2.2: Channel model.

The central question being explored is whether performance gains can be achieved when the receiver obtains knowledge of the channel state Ψ from an external sensor which we shall call “vision”. The specifics of the sensor are not relevant to the problem at hand; the importance instead lies in the fact that knowledge is obtained about the wireless channel beyond that which the transmitter and receiver can perceive in their default RF domain.

2.2.1 Cases Involving Varying Levels of Knowledge

Figure 2.2 depicts the simple scenario laid out here where the receiver obtains knowledge of the LOS state by some external means. To provide a comprehensive analysis of the effects of this vision on detection performance, we establish 3 distinct cases representing varying degrees of knowledge about the channel state, ordered by decreasing quality: (1) labeled knowledge (Vision), (2) statistical knowledge, (3) blind. In the *labeled* case the receiver obtains, at any point in time, an exact label of LOS or NLOS corresponding to the channel state Ψ such that the observed state, denoted $\hat{\Psi}$, matches the true state at all times, $\hat{\Psi}(t) = \Psi(t) \forall t$. This case is termed the “vision” case because it represents the use of external sensor-based information. In the *statistical* case the receiver no longer has access to labels for the channel state; rather, it merely has knowledge of the statistics of the channel model. (2.2) provides the marginal probability mass function for the channel state Ψ which follows a Bernoulli distribution parameterized by q , the probability of LOS. Finally, the *blind* case represents a lack of any information regarding the channel state at the receiver beyond

the *a priori* knowledge of the two possible amplitude values α_1 and α_2 , the signal shape $P(t)$, and the noise variance σ_n^2 . In the *blind* case the receiver has no notion of how often the channel is LOS vs NLOS, much less what the state is at any point in time.

One important characteristic distinguishing these cases is whether the information they provide is time-dependent. The vision case falls into this category as the labels provide an estimate of the channel state at any time t . The other two, however, give only model-specific information independent of time. This distinction is key to determining the achievable gains under different detection paradigms.

2.3 Detection Framework

To determine the presence of a signal with maximum reliability, one must construct a detector for which an input of N samples represented by the vector $\vec{r}(k)$ yields a decision upon whether the signal is present. Knowing this, there are two primary angles from which one can approach this detection problem. These two perspectives concern the number of hypotheses that are considered by the receiver, and in turn the methodology used to derive the optimal detection scheme. In one point of view, one can establish three hypotheses representing the no-signal, NLOS-signal, and LOS-signal states:

$$\begin{aligned}
 \mathcal{H}_0 &: A_s = 0 \text{ [No-Signal]} \\
 \mathcal{H}_1 &: \Psi = 0 \wedge A_s = \alpha_1 \text{ [NLOS Signal]} \\
 \mathcal{H}_2 &: \Psi = 1 \wedge A_s = \alpha_2 \text{ [LOS Signal]}
 \end{aligned} \tag{2.3}$$

In a second point of view, only two hypotheses are considered, one for the no-signal state and one for the signal-present state regardless of LOS:

$$\begin{aligned}\mathcal{H}_0 : A_s &= 0 \text{ [No-Signal]} \\ \mathcal{H}_1 : A_s &\neq 0 \text{ [Signal-Present]}\end{aligned}\tag{2.4}$$

Although these two models require different methodologies to arrive at the optimal detector, the ultimate decision rule that results must decide between the same two outcomes: signal-absent or signal-present. Intriguingly, it is shown in the following sections that these two models and approaches lead to the same optimal detection rule.

2.3.1 M -ary Detection using Bayes Risk

The 3-hypothesis model shown in (2.3) is an M -ary hypothesis testing problem, and it can be shown that having more than two hypotheses requires some *a priori* knowledge of the probabilities of these hypotheses occurring. If one takes the Neyman-Pearsonian approach, for example, comparing the likelihoods for each hypothesis requires more than one threshold; i.e. only two can be compared in a ratio test at one time. This leads us to formulate the Bayes Risk which considers the cost associated with every possible observation conditioned on the truth. Bayes Risk is defined in the most general case as follows:

$$\mathcal{R} = \sum_{i=0}^{M-1} \sum_{j=0}^{M-1} C_{ij} P(\mathcal{H}_i | \mathcal{H}_j) P(\mathcal{H}_j).\tag{2.5}$$

where $P(\mathcal{H}_i | \mathcal{H}_j)$ is the probability of choosing \mathcal{H}_i given that \mathcal{H}_j matches reality. The coefficients C_{ij} can be seen as weights which determine the contribution to the overall risk when making a decision \mathcal{H}_i conditioned on the truth, \mathcal{H}_j .

Minimization of the Bayes Risk encompasses any possible metric one might have for opti-

mality as it allows for arbitrary weight to be placed on Type-I and Type-II errors, otherwise known as *missed-detections* and *false-alarms* as they will henceforth be referred to. The interest in the problem at hand is in finding a detection rule which minimizes the probability of error or $\min_{\mathcal{H}_i}(P_e)$ where false-alarms and missed-detections are considered equally detrimental to the risk.

It has been shown that Bayes Risk is minimized if one decides \mathcal{H}_i for which $c_i(X) = \sum_{j=0}^{N-1} C_{ij}\pi(\mathcal{H}_j|X)$ is minimal where $\pi(\mathcal{H}_j|X)$ is the posterior probability of \mathcal{H}_j given an observation X . The optimal decision rule follows, upon definition of the weights C_{ij} . Adopting the $\min_{\mathcal{H}_i}(P_e)$ metric, the scenario at hand defines an error as mistaking the presence of a signal (\mathcal{H}_1 or \mathcal{H}_2) for the absence of a signal (\mathcal{H}_0) or equivalently in reverse. We can construct the C_{ij} matrix based off of this rule as follows:

$$C_{ij} = \begin{pmatrix} 0 & 1 & 1 \\ 1 & 0 & 0 \\ 1 & 0 & 0 \end{pmatrix} \quad (2.6)$$

where i indicates the decision index and j indicates the truth index. The symmetry of this matrix reflects the equal treatment of missed-detections and false-alarms, and the lack of risk associated with mistaking a LOS signal with an NLOS signal is represented with $C_{12} = C_{21} = 0$. Using this definition to minimize (2.5) leads to the following:

$$\underbrace{\operatorname{argmin}}_i [c_i(X)] = \left\{ \begin{array}{ll} \sum_{j=0}^2 \pi(\mathcal{H}_j|X) - \pi(\mathcal{H}_0|X) & i = 0 \\ \sum_{j=0}^2 \pi(\mathcal{H}_j|X) - \pi(\mathcal{H}_1|X) - \pi(\mathcal{H}_2|X) & 1 \text{ or } 2 \end{array} \right\} \quad (2.7)$$

The decision rule which minimizes \mathcal{R} then follows:

$$\begin{aligned} & \text{Choose } \mathcal{H}_i \text{ where} \\ i = & \left\{ \begin{array}{ll} 0 & \pi(\mathcal{H}_0|X) > \pi(\mathcal{H}_1|X) + \pi(\mathcal{H}_2|X) \\ 1 \text{ or } 2 & \text{otherwise} \end{array} \right\} \end{aligned} \quad (2.8)$$

This result resembles the classical *maximum a posteriori* (MAP) formulation for binary hypothesis testing with the key distinction being the union of \mathcal{H}_1 and \mathcal{H}_2 . It is now straightforward to obtain the decision rule in terms of the system parameters by substituting the likelihoods and priors associated with the three hypotheses.

$$\begin{aligned} & \text{Choose } \underbrace{\mathcal{H}_1 \text{ or } \mathcal{H}_2}_{\text{Signal Present}} \text{ if} \\ & L(X|\mathcal{H}_1)\pi_1 + L(X|\mathcal{H}_2)\pi_2 > L(X|\mathcal{H}_0)\pi_0 \end{aligned} \quad (2.9)$$

From (2.9) one can see the importance of knowledge of the prior probabilities $\{\pi_0, \pi_1, \pi_2\}$ in determining signal presence. Fortunately, although knowing the probability of the signal presence *a priori* might be impossible as in the case of radar, we have the privilege of knowing the probability of LOS, q , in the *vision* and *statistical* cases, though not the *blind*. Considering that $\pi_1 = (1 - q)(1 - \pi_0)$ and $\pi_2 = q(1 - \pi_0)$, the ratio $\frac{\pi_2}{\pi_1} = \frac{q}{1-q}$ is known for

these cases. This allows us to construct a decision rule where π_0 is the only unknown.

$$\begin{aligned}
& \text{Choose } \underbrace{\mathcal{H}_1 \text{ or } \mathcal{H}_2}_{\text{Signal Present}} \text{ if} \\
& e^{-\frac{1}{2\sigma_n^2} \sum_{k=0}^{N-1} (\bar{r}[k] - \alpha_1 \bar{P}[k])^2} (1 - q) + e^{-\frac{1}{2\sigma_n^2} \sum_{k=0}^{N-1} (\bar{r}[k] - \alpha_2 \bar{P}[k])^2} q \\
& > e^{-\frac{1}{2\sigma_n^2} \sum_{k=0}^{N-1} \bar{r}[k]^2} \frac{\pi_0}{1 - \pi_0} \\
& \exp \left[-\frac{1}{2\sigma_n^2} \left(\alpha_1^2 \sum_{k=0}^{N-1} \bar{P}[k]^2 - 2\alpha_1 \sum_{k=0}^{N-1} \bar{r}[k] \bar{P}[k] \right) \right] (1 - q) + \dots \\
& \exp \left[-\frac{1}{2\sigma_n^2} \left(\alpha_2^2 \sum_{k=0}^{N-1} \bar{P}[k]^2 - 2\alpha_2 \sum_{k=0}^{N-1} \bar{r}[k] \bar{P}[k] \right) \right] q > \underbrace{\frac{\pi_0}{1 - \pi_0}}_{\eta}
\end{aligned} \tag{2.10}$$

Now it can be seen that the sufficient statistic is a replica correlator, equivalent to a matched filter: $T(\bar{r}) = \sum_{k=0}^{N-1} \bar{r}[k] \bar{P}[k]$. The detection rule, however, cannot be isolated from the weight parameter q , indicating that knowledge of the probability of LOS is required for optimal detection performance.

2.3.2 Binary Composite Hypothesis Testing

As an alternative approach, one can consider only the two hypotheses shown in (2.4). A binary hypothesis testing scenario lends itself quite well to the Neyman-Pearsonian likelihood ratio test (LRT). Unlike the 3-ary Bayes risk approach, the binary approach requires treatment of the amplitude A_s as an unknown parameter and therefore falls into the category of detection of deterministic signals with unknown parameters. The LRT is optimal in that it maximizes the probability of detection (P_D) for a given probability of false alarm (P_{FA}) over all values of $A_s > 0$. The one-sided nature of this test, which results from the amplitude A_s being strictly positive, guarantees the existence of a UMP test. For more general scenarios

where A_s can be negative, different tests need to be used for the cases where A_s is positive or negative. In this setting we need only consider the positive case. [14, p.194] We can obtain the UMP detector by forming an LRT conditioned on A_s :

$$\begin{aligned} \text{Choose } \mathcal{H}_1 \text{ if } LRT(\vec{r}) &= \frac{L(\vec{r}; A_s, H_1)}{L(\vec{r}; H_0)} > \gamma, \\ \text{which implies } &\frac{\exp\left(-\frac{1}{2\sigma_n^2} \sum_{k=0}^{N-1} \left(\vec{r}[k] - A_s \vec{P}[k]\right)^2\right)}{\exp\left(-\frac{1}{2\sigma_n^2} \sum_{k=0}^{N-1} \vec{r}[k]^2\right)} > \gamma, \\ \rightarrow \sum_{k=0}^{N-1} \vec{r}[k] \vec{P}[k] &> \underbrace{\frac{A_s}{2} \sum_{k=0}^{N-1} \vec{P}[k]^2 - \frac{\sigma_n^2}{A_s} \log(\gamma)}_{\eta} \end{aligned} \quad (2.11)$$

The decision statistic obtained from the LRT is a replica correlator which notably does not depend on A_s . Further, although the threshold η does depend on A_s , this test is sufficient for a CFAR detection scheme even without knowledge of $\Psi(t)$ as the null (no-signal) hypothesis is independent of A_s .

If we return to the original interest in achieving $\min_{\mathcal{H}_i}(P_e)$ given knowledge of π_0 , the LRT is not sufficient without knowledge of A_s due to the power of the test (P_D) being dependent upon A_s . Instead the Bayesian approach to composite hypothesis testing comes into play, taking into account prior knowledge of the distribution of A_s which we possess in all knowledge cases except the *blind* case.

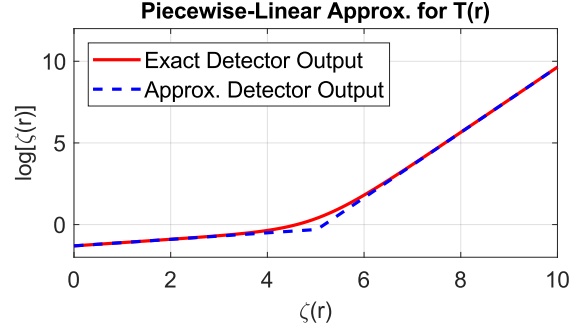


Figure 2.3: Piecewise-linear approximation vs exact detector.

The Bayes Factor for the scenario at hand has the following form:

Choose \mathcal{H}_1 if

$$\frac{\pi(\vec{r}; \mathcal{H}_1)}{\pi(\vec{r}; \mathcal{H}_0)} = \frac{\int_{\Omega_{A_s}} L(\vec{r}|A_s; \mathcal{H}_1)p(A_s; \mathcal{H}_1)dA_s}{\int_{\Omega_{A_s}} L(\vec{r}|A_s; \mathcal{H}_0)p(A_s; \mathcal{H}_0)dA_s} > \underbrace{\frac{\pi_0}{1 - \pi_0}}_{\eta}, \quad (2.12)$$

where $p(A_s; \mathcal{H}_1) = (1 - q)\delta(A_s - \alpha_1) + q\delta(A_s - \alpha_2)$,

$p(A_s; \mathcal{H}_0) = \delta(A_s)$,

$\delta(\cdot)$ is the Dirac Delta Function.

The Bernoulli form for the prior distribution on the amplitude A_s derives from the signal model shown in (2.2). The prior distribution for \mathcal{H}_0 is a point mass at zero representing the no-signal state. Applying these known priors yields a decision rule identical to that found in (2.10).

2.3.3 Performance Analysis

To evaluate the performance of this detection scheme we must derive expressions for probability of detection (P_D) and false-alarm (P_{FA}). One can either characterize the performance for a single observation or for an ensemble of observations, a distinction which emerges when

time-dependent information about the channel is available as in the *vision* case. Here we desire to optimize ensemble performance and utilize the detection scheme which minimizes the average P_e . An exact form for P_D and P_{FA} given an arbitrary q value, however, is not tractable due to the exponential mixture form of the decision statistic in (2.10). An approximation is therefore employed which utilizes a piecewise-linear function in place of the weighted sum of complex exponentials:

$$\begin{aligned}
T(\vec{r}) &= c_1 \exp(\Phi_1 \zeta(\vec{r})) + c_2 \exp(\Phi_2 \zeta(\vec{r})), \text{ where} \\
c_1 &= (1 - q) \exp\left(-\frac{\alpha_1^2 \epsilon(P)}{2\sigma_n^2}\right), \quad c_2 = q \exp\left(-\frac{\alpha_2^2 \epsilon(P)}{2\sigma_n^2}\right), \\
\Phi_1 &= \frac{\alpha_1}{\sigma_n^2}, \quad \Phi_2 = \frac{\alpha_2}{\sigma_n^2}, \quad \epsilon(P) = \sum_{k=0}^{N-1} \vec{P}[k]^2, \quad \zeta(\vec{r}) = \sum_{k=0}^{N-1} \vec{r}[k] \vec{P}[k]
\end{aligned} \tag{2.13}$$

We can then form the following piecewise-linear approximation for the logarithm of $T(\vec{r})$ with boundary B :

$$\begin{aligned}
\ln(T(\vec{r})) &\approx \begin{cases} \log(c_1) + \Phi_1 \zeta(\vec{r}) & \vec{r} \leq B \\ \log(c_2) + \Phi_2 \zeta(\vec{r}) & \vec{r} > B \end{cases} \\
c_1 e^{\Phi_1 B} = c_2 e^{\Phi_2 B} &\rightarrow B = \frac{\ln(\frac{c_2}{c_1})}{\Phi_1 - \Phi_2}
\end{aligned} \tag{2.14}$$

This yields an approximate decision rule as follows:

Choose \mathcal{H}_1 if

$$\left\{ \begin{array}{l} \{\zeta(\vec{r}) > \eta_1\} \cap \{\zeta(\vec{r}) \leq B\} \\ \text{or} \\ \{\zeta(\vec{r}) > \eta_2\} \cap \{\zeta(\vec{r}) > B\} \end{array} \right\}$$

where

(2.15)

$$\begin{aligned} \eta_1 &= \frac{\sigma_n^2}{\alpha_1} \log \left(\frac{\pi_0}{(1 - \pi_0)(1 - q)} \right) + \frac{\alpha_1 \epsilon(P)}{2} \\ \eta_2 &= \frac{\sigma_n^2}{\alpha_2} \log \left(\frac{\pi_0}{(1 - \pi_0)q} \right) + \frac{\alpha_2 \epsilon(P)}{2} \\ B &= \log \left(\frac{q}{1 - q} \right) \frac{\sigma_n^2}{\alpha_1 - \alpha_2} + \frac{\epsilon(P)}{2} \left(\frac{\alpha_1^2 - \alpha_2^2}{\alpha_1 - \alpha_2} \right) \end{aligned}$$

The approximation forms two decision rules with corresponding optimal thresholds, each assuming dominance of one channel state or the other. In approximation, expressions for P_D and P_{FA} are realizable, and using the fact that the decision statistic $\zeta(\vec{r})$ is a random variable with the following distribution: $\zeta(\vec{r}) \sim \mathcal{N}(A_s \epsilon(P), A_s^2 \sigma_n^2 \epsilon(P))$, one can obtain the ensemble P_D and P_{FA} expressions dependent on the two thresholds η_1 and η_2 and the boundary B as

follows:

$$\begin{aligned}
P_D &= Pr [\text{Choose signal-present} | \mathcal{H}_1] \\
P_D &= 1 \{ \eta_1 \leq B \} (Pr [\zeta(\vec{r}) > \eta_1 | A_s = \alpha_1] (1 - q) + \dots \\
&\quad Pr [\zeta(\vec{r}) > \eta_1 | A_s = \alpha_2] q) + \dots \\
&\quad 1 \{ \eta_1 > B \} (Pr [\zeta(\vec{r}) > \eta_2 | A_s = \alpha_1] (1 - q) + \dots \\
&\quad Pr [\zeta(\vec{r}) > \eta_2 | A_s = \alpha_2] q) \\
\rightarrow P_D &= \\
1 \{ \eta_1 \leq B \} &\left[Q \left(\frac{\eta_1 - \alpha_1 \epsilon(P)}{\sigma_n \sqrt{\epsilon(P)}} \right) (1 - q) + Q \left(\frac{\eta_1 - \alpha_2 \epsilon(P)}{\sigma_n \sqrt{\epsilon(P)}} \right) q \right] \\
+ 1 \{ \eta_1 > B \} &\left[Q \left(\frac{\eta_2 - \alpha_1 \epsilon(P)}{\sigma_n \sqrt{\epsilon(P)}} \right) (1 - q) + Q \left(\frac{\eta_2 - \alpha_2 \epsilon(P)}{\sigma_n \sqrt{\epsilon(P)}} \right) q \right] \\
P_{FA} &= Pr [\text{Choose signal-present} | \mathcal{H}_0] \\
\rightarrow P_{FA} &= \\
1 \{ \eta_1 \leq B \} &Q \left(\frac{\eta_1}{\sigma_n \sqrt{\epsilon(P)}} \right) + 1 \{ \eta_1 > B \} Q \left(\frac{\eta_2}{\sigma_n \sqrt{\epsilon(P)}} \right)
\end{aligned} \tag{2.16}$$

The piecewise-approximate detector has piecewise expressions for P_D and P_{FA} where the boundary condition is a comparison between one of the thresholds (η_1 or η_2) and B , all of which depend on the estimate for probability of LOS, \hat{q} , the prior probability of signal presence, π_0 , and otherwise known parameters.

2.4 Case-Based Analysis

The generalized detection scheme shown in (2.15) assumes some knowledge of q at the receiver, denoted \hat{q} , and it is this knowledge which differs among the three cases presented. The weights for the terms in the P_D and P_{FA} expressions depend on the true value of q while the thresholds η_1 and η_2 as well as the boundary B depend on the known value at the receiver, \hat{q} . Each knowledge case modifies its definition of \hat{q} , thereby altering the chosen thresholds.

2.4.1 Labeled Knowledge (Vision)

In the case where external knowledge of the LOS state Ψ is available, the knowledge at the receiver is binary in nature, meaning that \hat{q} is either equal to 1 when the label is LOS or 0 when the label is NLOS. The expressions for P_D and P_{FA} for the vision case are then as follows:

$$\begin{aligned} P_{D-V} &= Q\left(\frac{\eta_1 - \alpha_1 \epsilon(P)}{\sigma_n \sqrt{\epsilon(P)}}\right) (1 - q) + Q\left(\frac{\eta_2 - \alpha_2 \epsilon(P)}{\sigma_n \sqrt{\epsilon(P)}}\right) q \\ P_{FA-V} &= Q\left(\frac{\eta_1}{\sigma_n \sqrt{\epsilon(P)}}\right) (1 - q) + Q\left(\frac{\eta_2}{\sigma_n \sqrt{\epsilon(P)}}\right) q \end{aligned} \quad (2.17)$$

P_D and P_{FA} for the vision case are exact results and do not rely on the piecewise-linear approximation because only one term in the weighted sum of exponentials need be considered at a time.

2.4.2 Statistical Knowledge

In the case where the receiver no longer has access to the labeled LOS state, \hat{q} is simply equal to the true probability of LOS for the channel. This yields the following expressions

for P_D and P_{FA} :

$$\begin{aligned}
P_{D-S} &= \\
& 1 \{ \eta_1 \leq B \} \left[Q \left(\frac{\eta_1 - \alpha_1 \epsilon(P)}{\sigma_n \sqrt{\epsilon(P)}} \right) (1 - q) + Q \left(\frac{\eta_1 - \alpha_2 \epsilon(P)}{\sigma_n \sqrt{\epsilon(P)}} \right) q \right] + \\
& 1 \{ \eta_1 > B \} \left[Q \left(\frac{\eta_2 - \alpha_1 \epsilon(P)}{\sigma_n \sqrt{\epsilon(P)}} \right) (1 - q) + Q \left(\frac{\eta_2 - \alpha_2 \epsilon(P)}{\sigma_n \sqrt{\epsilon(P)}} \right) q \right] \quad (2.18)
\end{aligned}$$

$$\begin{aligned}
P_{FA-S} &= \\
& 1 \{ \eta_1 \leq B \} Q \left(\frac{\eta_1}{\sigma_n \sqrt{\epsilon(P)}} \right) + 1 \{ \eta_1 > B \} Q \left(\frac{\eta_2}{\sigma_n \sqrt{\epsilon(P)}} \right)
\end{aligned}$$

For the *statistical* case this result is an approximation as the entire distribution with both LOS and NLOS terms must be considered.

2.4.3 Blind

In the absence of even statistical knowledge of the channel, the receiver's knowledge of LOS is entirely non-existent. The best strategy is therefore to establish an uninformative prior distribution on the parameter \hat{q} . Considering that the distribution for q is known to be Bernoulli even in the blind case, a good choice for the prior on \hat{q} is the Beta $(\frac{1}{2}, \frac{1}{2})$ distribution. The ensemble performance can then be found by marginalizing the original

Bayes Factor from (2.12) over the entire space of \hat{q} such that its dependence is removed:

Choose \mathcal{H}_1 if

$$\frac{\pi(\vec{r}; \mathcal{H}_1)}{\pi(\vec{r}; \mathcal{H}_0)} = \frac{\int_{\hat{q}=0}^1 \int_{\Omega_{A_s}} L(\vec{r}|A_s; \mathcal{H}_1) p(A_s|\hat{q}; \mathcal{H}_1) dA_s d\hat{q}}{\int_{\hat{q}=0}^1 \int_{\Omega_{A_s}} L(\vec{r}|A_s; \mathcal{H}_0) p(A_s|\hat{q}; \mathcal{H}_0) dA_s d\hat{q}} > \underbrace{\frac{\pi_0}{1 - \pi_0}}_{\eta}, \quad (2.19)$$

$$\text{where } p(A_s|\hat{q}; \mathcal{H}_1) = (1 - \hat{q})\delta(A_s - \alpha_1) + \hat{q}\delta(A_s - \alpha_2),$$

$$p(A_s|\hat{q}; \mathcal{H}_0) = \delta(A_s),$$

$\delta(\cdot)$ is the Dirac Delta Function.

This yields an identical decision rule to (2.15) but with $q = 0.5$. Therefore, in the absence of statistical knowledge, the receiver should assume equal weighting between LOS and NLOS channel states. The expressions for P_D and P_{FA} for the blind case are then as follows:

$$\begin{aligned} P_{D-B} = & \\ & 1 \{ \eta_1 \leq B \} \left[Q \left(\frac{\eta_1 - \alpha_1 \epsilon(P)}{\sigma_n \sqrt{\epsilon(P)}} \right) (1 - q) + Q \left(\frac{\eta_1 - \alpha_2 \epsilon(P)}{\sigma_n \sqrt{\epsilon(P)}} \right) q \right] \\ & + 1 \{ \eta_1 > B \} \left[Q \left(\frac{\eta_2 - \alpha_1 \epsilon(P)}{\sigma_n \sqrt{\epsilon(P)}} \right) (1 - q) + Q \left(\frac{\eta_2 - \alpha_2 \epsilon(P)}{\sigma_n \sqrt{\epsilon(P)}} \right) q \right] \end{aligned} \quad (2.20)$$

$$P_{FA-B} = 1 \{ \eta_1 \leq B \} Q \left(\frac{\eta_1}{\sigma_n \sqrt{\epsilon(P)}} \right) + 1 \{ \eta_1 > B \} Q \left(\frac{\eta_2}{\sigma_n \sqrt{\epsilon(P)}} \right)$$

$$\text{With } \hat{q} = \frac{1}{2}.$$

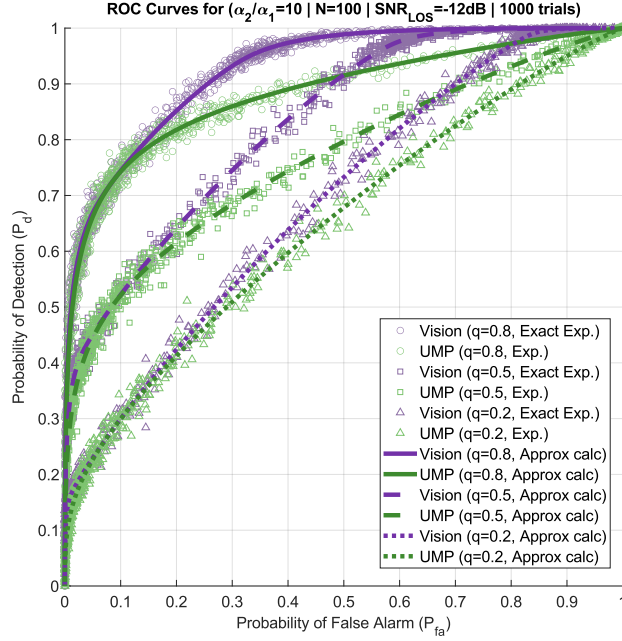


Figure 2.4: ROC curve (CFAR) performance: vision vs UMP test.

2.5 Numerical Results and Discussion

Here these performance results are tested under both CFAR and $\min_{\mathcal{H}_i}(P_e)$ detection paradigms in a Monte Carlo simulation. Beginning with the CFAR detection simulation, $T = 1000$ trials are performed in which $N = 100$ samples are collected from a received signal with arbitrary known shape. For each trial, a signal-present scenario and a signal-absent scenario are tested, and the exact decision rule shown in (2.10) is used to determine the receiver's hypothesis of choice. This process is performed over a range of prior π_0 values producing the receiver operating characteristic (ROC) shown in Figure 2.4. Note that the *statistical* and *blind* cases produce performance identical to the UMP test from a ROC perspective, and thus only a comparison between *vision* and UMP is necessary.

The probability of error simulation is performed in a similar fashion, but the trials are performed while sweeping over SNR values and a fixed value of $\pi_0 = 0.5$. Note that the average SNR is calculated as $\text{SNR}_{avg} = \frac{\epsilon(P)((1-q)\alpha_1^2 + q\alpha_2^2)}{\sigma_n^2}$.

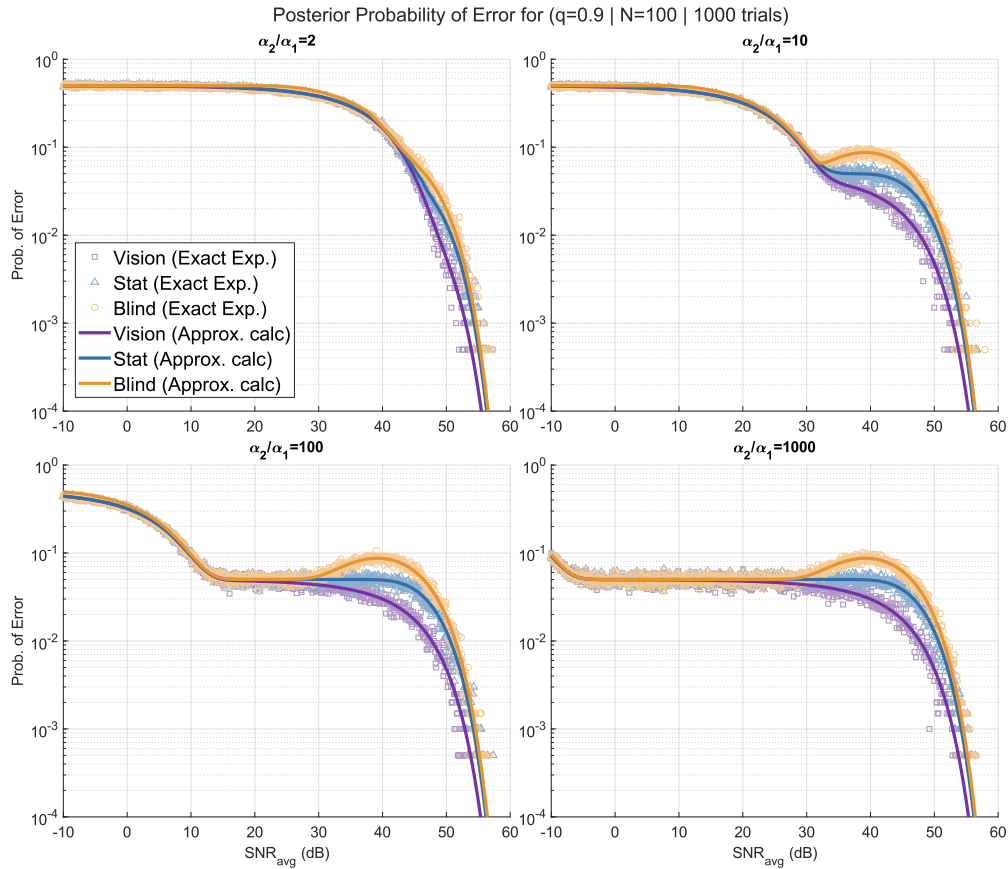


Figure 2.5: Prob. of error performance: vision vs statistical vs blind

One can see from the ROC curves that the *vision* case always provides a higher P_D for a given P_{FA} than the UMP test, and the gain achieved depends upon the probability of LOS, q . This sets the *vision* case apart from the other knowledge cases. The benefit provided by the *statistical* case over the *blind* case is demonstrated in the prob. of error curves wherein prior knowledge of signal presence is available.

2.6 Conclusions and Future Work

We have shown that information provided through sensors which is supplementary to that obtained by the receiver itself can, under the right circumstances, improve the detection

performance for the receiver when a dynamic detection scheme is used. Moreover, out of three knowledge cases presented, *vision*, *statistical*, and *blind*, the *vision* case leads to better ensemble performance compared to the UMP test while the others do not. By dynamically changing the detection threshold used depending on the known channel state, one can allow higher false alarm rates in NLOS conditions while lowering false alarm rates in LOS conditions to achieve the desired average false alarm rate. Possession of statistical knowledge at the receiver, although not helpful in a CFAR paradigm, dominates the *blind* case when prior information about signal presence is provided.

The results obtained point to the broader advantage provided by sensor-based information for both CFAR and $\min_{\mathcal{H}_i}(P_e)$ detectors. Therefore, future work should examine the impact of imperfect sensor-based information, a scenario more representative of real systems. There is also ample room to explore the impact of *vision* for more sophisticated channels such as those with Rayleigh and Ricean fading.

Chapter 3

Optimal Performance of Vision Sensor-Aided Receivers with Imperfect Information

3.1 Introduction

Our increasingly interconnected world demands a rapidly growing fleet of sensors of all kinds, spread throughout our daily lives. The phenomenon of Internet of Things (IoT) has so infiltrated the information space that the number of mobile users of cellular networks worldwide is expected to reach 80 billion by 2030 [24]. This incredible figure reflects the need for IoT-enabled sensors to reliably communicate via wireless sensor networks, enabling intelligent automation for the home, healthcare (e-health), transportation systems (ITS), farms, and the military among sundry other industries [25]. Meteorological sensors, microphones, optical and infra-red (IR) cameras, LiDARs, radars, and countless other varieties are increasingly becoming standard components of mobile-connected devices such as smartphones and vehicles as well as stationary devices such as WiFi access points, street lights, cellular base stations, and electric meters. Furthermore, the fidelity and information content provided by these sensors is set to rise with the advent of sixth-generation (6G) cellular networks and their incorporation of augmented reality and autonomous driving systems [26].

IoT-based sensors are often found in highly dynamic environments such as urban roadways where the spatial properties of the wireless channel can change on a millisecond basis. The value of out-of-band information, which can often include that provided through optical and IR sensors, is especially present in these types of environments. The literature has provided a number of examples where existing RF communications systems achieve performance benefits from the incorporation of external information. In millimeter wave systems, for instance, where estimating the spatial covariance is necessary for link configuration, an out-of-band sub-6 GHz channel has been shown to reduce training overhead and increase data rates [12, 13, 27]. The integration of radar- or camera-based sensing capabilities with communications systems can also jointly improve localization and imaging capabilities while simultaneously reducing overhead or improving physical layer performance [6, 28]. Cameras combined with computer vision technology have also been utilized to provide spatial information for beamforming, blockage detection, localization, and other sensing typically performed by the existing RF system [29, 30].

The application of out-of-band and otherwise external knowledge to the most fundamental principles of RF signal detection is the crux of the work presented here. Expanding upon Chapter 2, we lay out a framework for the detection of RF signals in additive white Gaussian noise (AWGN) which incorporates a two-state channel exhibiting either line-of-sight (LOS) or non-line-of-sight (NLOS) conditions. Our major contributions lie in the benefits garnered from obtaining knowledge at the receiver about the NLOS/LOS channel from an external sensor, which we refer to as *vision*, compared to baseline approaches without vision information. This chapter extends the analysis of Chapter 2 by providing a continuous-time-Markov-Chain (CTMC) channel model through which the detection framework presented can be tuned to a variety of realistic scenarios yielding vision information with varying degrees of fidelity and reliability.

3.1.1 Prior Work

We approach this problem from the standpoint of classical detection theory and hypothesis testing and challenge the traditional maximum likelihood estimation and universally-most-powerful (UMP) test when time-dependent knowledge is available. Chapter 2 is the underpinning of this analysis wherein we present three cases of NLOS/LOS knowledge, termed *vision*, *statistical*, and *blind*, and show analytically and experimentally how the *vision* case can improve upon the performance of the UMP test in an ensemble of trials in a constant-false-alarm-rate (CFAR) paradigm. In this chapter, we provide a more detailed analysis behind the ability for dynamic detection schemes to out-perform static schemes such as the UMP test and greatly expand the concept of vision information, allowing for imperfect vision where sensor-based information is only sporadically available.

The signal detection scenario we present features hypotheses without fully-known distributions and, therefore, unknown parameters must be accounted for when obtaining the optimal decision rule. The literature provides two approaches which address the unknown parameter detection problem from different angles; namely, the m -ary hypothesis approach and the composite hypothesis approach [14]. The latter is further broken down into the generalized likelihood ratio test (GRLT), Rao, and Wald tests which are asymptotically optimal for MLE estimates of the unknown parameter(s) with independent and identically-distributed (IID) data [15, 16, 17]. The GRLT, Rao, and Wald tests, however, do not take into account prior knowledge of the distribution of the parameter itself whereas the Bayesian composite hypothesis testing method does [18, 19, 20]. As this prior distribution is known in the problem at hand, it should logically be factored into the detection scheme.

The preliminary work in Chapter 2 treats the received signal amplitude as an unknown parameter whose state can be optionally obtained through a label, corresponding to the

increased path loss experienced in NLOS conditions. This parameter is a Bernoulli random variable resembling the characterization used in [21]. [22] provides another application in which a mixed NLOS/LOS environment is considered. The legitimacy of the uniformly-most-powerful (UMP) test is challenged for cases where the test statistic does not depend on the unknown parameter [23]. In the scenario presented, even though a UMP test does exist in a (CFAR) detection paradigm, it is shown that, by adopting a dynamic detection scheme, one can achieve a higher probability of detection over an ensemble of trials for a given false alarm rate than that achieved through the UMP test. Furthermore, given prior probabilities for the hypotheses, one can achieve a lower overall probability of error given knowledge of the parameter distribution than without knowledge, even if this knowledge is unchanging and time-independent.

The detection framework presented here is based on the stochastic properties of the binary CTMC channel model, which is closely related to the Gilbert-Elliott channel model. In the Gilbert-Elliott model, a stationary, discrete, binary Markov process is used to define good and bad states for the channel which typically correspond to lower and higher SNR values. The Markovian nature of Gilbert Elliott introduces memory due to the dependence of current states on previous states [31], a property shared by the binary CTMC used in this work. Additionally, the CTMC can be thought of as a variation on the finite state Markov channel (FSMC) where only two states are used and, crucially, instead of defining discrete intervals as is often done [32], the CTMC is a continuous random process featuring stochastic holding times [33].

3.1.2 Contributions and Problem Setup

This work explores the impact of external sensor-based information on wireless communication and radar receivers and answers the question of whether and how valuable this information could be. More specifically, if information is obtained about the channel LOS/NLOS state beyond that which can be obtained in the radio frequency band of operation, how and to what degree can detection performance be improved?

There are two settings within which this detection problem resides, namely: the constant false-alarm rate (CFAR) detection paradigm and the minimum probability of error (\min_{P_e}) paradigm. The first concerns situations where the occurrence of an event must be detected without prior knowledge of the probabilities of its occurrence or the occurrence of alternative events. The \min_{P_e} paradigm refers to situations where the probability of an event's occurrence as well as the occurrence of alternative events is known a-priori, and the probability of incorrect detection (error) is minimized. The CFAR paradigm lends itself well to radar applications as the probability of the target's presence is seldom known in advance. The \min_{P_e} paradigm is well-suited for digital communications systems as the symbol probabilities are usually known a-priori.

This chapter makes the following contributions:

- A binary CTMC channel model is introduced which characterizes intermittent toggling between line-of-sight and non-line-of-sight states. The decision statistic for on-off-keying (OOK) signals passing through the CTMC channel is presented along with its detection and false-alarm probabilities under varying degrees of knowledge.
- A generalized detection framework is laid out which minimizes the probability of error using a Bayes Risk formulation. The framework features an optimal decision rule which

can be applied with any type of time-dependent or static knowledge sourced from a vision sensor regarding the NLOS/LOS state. We show that dynamic detectors which adjust their decision rule based upon labeled channel information can out-perform static detectors in an ensemble of trials. Moreover, we prove that any static detector will achieve identical performance to the UMP test under the CFAR paradigm.

- An optimal decision rule is presented for receivers with imperfect vision information which is prone to error and available only available at certain points in time. It is shown that the cases of *perfect vision* and *statistical* knowledge are special cases of a more general *periodic labels* model wherein samples of the NLOS/LOS channel, subject to error, are sent to the receiver at set intervals. The performance of such imperfect vision receivers is shown to lie between that of the UMP test and that of *perfect vision*.

3.2 System Model

Here we expand upon the scenario presented in Chapter 2 by establishing a continuous-time model for the NLOS/LOS channel. Similarly, in this scenario a receiver must detect the presence of a signal with known pulse shape in an AWGN channel. The attenuation incurred by this channel is stochastic in nature, also consistent with the Chapter 2. However, the state of the channel, $\Psi(t)$, is described in a far more specific way as a continuous-time random process. The signal of interest (SOI) is also modeled as a continuous-time random process but one independent from that of the channel state $\Psi(t)$.

Focusing first on the signal model, the SOI follows a random process whose continuous-time properties need not be fully described, but its stationary distribution is important. The stationary distribution describes the binary state of the signal, either present leading to a positive amplitude or absent leading to an amplitude of zero. The received signal $r(t)$ is

composed of the transmit signal $s(t)$ scaled by the channel value $h(t)$ and the addition of a white Gaussian noise process $n(t)$ with variance σ_n^2 . The received signal is then sampled, bringing the signal representation into discrete-time.

$$\text{c.t.: } r(t) = s(t)h(t) + n(t)$$

$$\text{d.t.: } \vec{r}(k) = \vec{s}(k)\vec{h}(k) + \vec{n}(k)$$

where

$$n_k \sim \mathcal{N}(0, \sigma_n^2), \quad s_k \sim f_{s_k}(s) = \left\{ \begin{array}{ll} \pi_0, & s = 0 \\ 1 - \pi_0, & s = P_k \end{array} \right\} \quad (3.1)$$

$$0 \leq k \leq N$$

The signal itself consists of a pulse shape $P(t)$ with $0 \leq t \leq T_P$, and this pulse shape is assumed to be known at the receiver. The observation made by the receiver is a vector of N samples taken at a particular sample rate, f_s , and, crucially, the receiver is assumed to be time-aligned with the transmit pulse. The N samples observed at the receiver correspond to the pulse samples $P(k)$, $\{0 \leq k \leq N - 1\}$ such that the sample index k represents the k^{th} sample of the pulse. The marginal distribution for the transmit signal shown in (3.1) has support on $\{0, P_k\}$ and involves the value π_0 which is the probability of signal absence. In the CFAR paradigm π_0 is not known at the receiver, but in the $\min(P_e)$ paradigm it is.

Now turning our attention to the channel model, we can describe the underlying process governing the channel value $h(t)$ using the channel state $\Psi(t)$. The interest in this work lies in the impact from knowledge of a NLOS/LOS state, and that state is represented as two possible channel values, $h(t) \in \{\alpha_1, \alpha_2\}$ corresponding to a lower channel gain α_1 for NLOS conditions and a higher channel gain α_2 for LOS conditions. The assumption is made that $\alpha_2 > \alpha_1 \forall t$. In this model the channel toggles between NLOS and LOS states intermittently,

taking on the lower or higher amplitude accordingly. The channel state, $\Psi(t)$, takes on values of 0 and 1 for the NLOS and LOS states. The channel value is then related to the state as follows: $h(t) = (1 - \Psi(t))\alpha_1 + \Psi(t)\alpha_2$.

$\Psi(t)$ is governed by a binary continuous-time Markov chain (CTMC). This models a channel which experiences non-line-of-sight (NLOS) and line-of-sight (LOS) conditions in a dynamic way such that the expected received signal amplitude toggles between a lower value α_1 and a higher value α_2 with $\alpha_2 > \alpha_1$, corresponding to the values $\Psi(t) = 0$ and $\Psi(t) = 1$, respectively. The CTMC is characterized by the distribution of the duration of each channel state period, referred to henceforth as the holding times.

The definition of the CTMC involves exponentially distributed, independent holding times: $E_0 \sim \text{Exp}(\lambda_0)$ and $E_1 \sim \text{Exp}(\lambda_1)$ corresponding to the NLOS and LOS channel states, with $E_0 \perp\!\!\!\perp E_1$. The rate parameters λ_0 and λ_1 determine the mean holding times: $\mathbb{E}\{E_0\} = \frac{1}{\lambda_0}$, $\mathbb{E}\{E_1\} = \frac{1}{\lambda_1}$. After each holding period, the process switches to the other state with 100% probability. As this is a binary CTMC, there is only one alternative state to switch to after each holding period, and there is no chance of remaining in the current state.

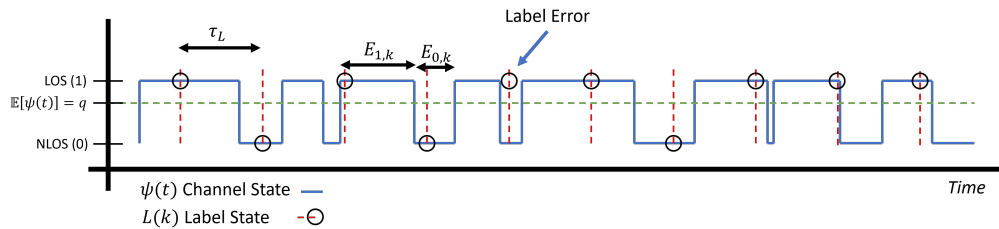


Figure 3.1: CTMC channel and label processes over time

There are several important properties of the CTMC process that will be relevant later in this work. The first is the stationary distribution which involves the mean of the process, $\mathbb{E}\{\Psi(t)\}$. The stationary distribution can be found from the generator matrix Q defined as

follows:

$$Q_\Psi = \begin{bmatrix} -\lambda_0 & \lambda_0 \\ \lambda_1 & -\lambda_1 \end{bmatrix} \quad (3.2)$$

The off-diagonal elements of Q are the rate parameters for the holding times described earlier. The stationary distribution can describe the probabilities of the process being in each state after infinite time has elapsed, and it satisfies the following linear relationship: $\bar{\pi}Q = 0$. Solving this yields the following stationary probabilities: $\bar{\pi} = \begin{bmatrix} \frac{\lambda_1}{\lambda_0 + \lambda_1} & \frac{\lambda_0}{\lambda_0 + \lambda_1} \end{bmatrix}$ which correspond to the stationary probability of NLOS and LOS. For ease of notation, the stationary probability of LOS will henceforth be referred to as $q = \frac{\lambda_0}{\lambda_0 + \lambda_1}$. The mean of the CTMC can be described as $\mathbb{E}\{\Psi(t)\} = \sum_{i=0}^1 i\bar{\pi}_i = \frac{\lambda_0}{\lambda_0 + \lambda_1} = q$. This is conveniently equivalent to the stationary probability of LOS.

An example realization of the CTMC channel process is depicted in Figure 3.1. In this example the channel spends slightly more time in the LOS state than it does in the NLOS state, corresponding to a mean value greater than 1/2. The number of jumps in any finite time period is related to the rate parameters λ_0 and λ_1 . In general, larger rate parameters lead to a faster changing channel while smaller values lead to infrequent jumps. Furthermore, the ratio between parameter values determines the preference towards the NLOS or LOS state.

$$\begin{aligned} r_k \sim f_{r_k} &= \pi_0 \left\{ \frac{1}{\sqrt{2\pi\sigma_n^2}} e^{-\frac{r_k^2}{2\sigma_n^2}} \right\} + \dots \\ &(1 - \pi_0)(1 - q) \left\{ \frac{1}{\sqrt{2\pi\sigma_n^2}} e^{-\frac{1}{2\sigma_n^2}(r_k - \alpha_1 P_k)^2} \right\} + \dots \\ &(1 - \pi_0)q \left\{ \frac{1}{\sqrt{2\pi\sigma_n^2}} e^{-\frac{1}{2\sigma_n^2}(r_k - \alpha_2 P_k)^2} \right\} \end{aligned} \quad (3.3)$$

The received signal, after passing through the CTMC channel and being impaired with AWGN noise, takes on the marginal distribution shown in (3.3). This is best characterized as a Gaussian mixture with weights determined by q and the prior probability of the null

hypothesis, π_0 .

3.2.1 Knowledge at the Receiver

The central feature of dynamic detection being explored in this work is the availability of time-dependent channel knowledge at the receiver. This knowledge can take on several different forms, and these types of knowledge are outlined here. In the Chapter 2 we outlined three cases: the *vision* case, the *statistical* case, and the *blind* case wherein the first case involves knowledge of the channel state at all times, the second involves knowledge of the probability of LOS, and the third involves a lack of any knowledge regarding the LOS state. This work expands the realm of knowledge that could be available at the receiver and its relationship to time.

Channel knowledge can be categorized in terms of its temporal availability as well as its fidelity. Some knowledge, like that obtained from an external sensor, is time-dependent, giving the receiver information about the evolution of the channel state. In other cases, the knowledge is time-independent, providing information about the stationary properties of the channel such as the probability of LOS, q . We will denote the former as “labeled” knowledge and the latter as “unlabeled”. This contrast can be illustrated by considering that, with an external sensor, the receiver can obtain temporally relevant information about the channel whereas, without an external sensor, the receiver can only obtain statistical information unchanging with time.

Labeled knowledge, which is of particular interest in this chapter, can then be further broken down based upon the temporal relevance of the labels. In the ideal case, the receiver obtains knowledge of the exact channel state at all times. This is precisely the *vision* case outlined in the Chapter 2. More generally, however, a sensor may provide labels only at specific points

in time, or discontinuously, reminiscent of pilot symbols in traditional channel estimation. We will refer to evenly-spaced labeled knowledge as periodic labels. The spacing between the labels need not be even, but for the purposes of this work we will assume they are periodic. Although periodic labels do provide time-dependent information, this information is potentially outdated and serves as a form of memory.

Another crucial knowledge property to consider is the fidelity of the labels which can be thought of as their susceptibility to error. All real-world sensors will incur errors in their measurements, and the impact of these errors on the usefulness of labeled knowledge is examined in this work. An external sensor in a communication system can be modeled as having a channel of its own in addition to the primary RF data channel. Rather than modeling this side channel, we assume that the label error rate is known, and label errors correspond to perceived LOS states while the true state is NLOS or vice-versa. Labeled knowledge with an error rate less than one will be referred to as imperfect labels.

The CTMC channel realization in Figure 3.1 includes a series of imperfect periodic labels spaced out by periods of τ_L time units. One label error is shown in this realization as a label inconsistent with the current channel state. The labels form a random process themselves which we takes on the following marginal distribution: $L(k) \sim f_{l_k}(l_k) = \left\{ \begin{array}{ll} 1 - \epsilon, & l_k = \Psi(t_k) \\ \epsilon, & l_k = 1 - \Psi(t_k) \end{array} \right\}$ where ϵ is the probability of label error and t_k is the time-tamp for the k_{th} label. The label process can also be defined directly as a function of the channel state process and an independent Bernoulli error process: $L(k) = \Psi(t_k) \oplus \zeta(k)$ where \oplus denotes the modulo-two addition operator and $\zeta(k) \sim \text{Bernoulli}(\epsilon)$.

As a final knob, one can consider whether the channel parameters; i.e., the rate parameters λ_0 and λ_1 , are available at the receiver. The statistical case in the Chapter 2 corresponds to unlabeled knowledge of the stationary probability of LOS, q , and the blind case involves

a lack of any knowledge about the LOS state, either labeled or unlabeled. Here we expand this concept to the case of periodic labels wherein blind periodic labels implies that the stationary channel properties are not available at the receiver. Since $q = \frac{\lambda_0}{\lambda_0 + \lambda_1}$ is defined in terms of these parameters, its availability is implied if the rate parameters are available.

By manipulating the parameters discussed such as the label spacing τ_L , label error rate ϵ , and the availability of the rate parameters, we can gain a comprehensive understanding of the performance benefits garnered from labeled knowledge and its value in more realistic settings.

3.3 Generalized Detection Framework

Having outlined the system model and described the types of knowledge available at the receiver, we can now turn our attention to the detection of the SOI and the performance we can expect in both CFAR and $\min(P_e)$ paradigms. The receiver must use its observation of N samples to make a decision upon whether the signal is present. This fundamental goal is identical to that described in [1] where we derived an optimal decision rule using two methodologies: M-ary detection using Bayes risk and binary composite hypothesis testing. To avoid redundancy, we will not repeat these derivations here, but rather connect their results to the expanded system model at hand.

In order to discuss the impact of labeled knowledge and its various forms, we must first establish a generalized decision rule which can be applied to each type of knowledge through a single parameter, \hat{q} . This parameter can be thought of as the estimated probability of LOS based on knowledge at the receiver, which should be differentiated from the true probability of LOS, q . The source of this parameter depends on the type of knowledge available, with labeled knowledge allowing \hat{q} to evolve with time and unlabeled knowledge producing a static

value for \hat{q} . In the ideal case, that of perfect *vision* outlined in [1], \hat{q} takes on only extreme values: $\hat{q} \in \{0, 1\}$ because the full LOS information is available at all times. Later in this work we will show that less-ideal forms of labeled knowledge such as imperfect periodic labels will also yield a time-varying \hat{q} .

$$\begin{aligned}
& \text{Choose } \underbrace{\mathcal{H}_1 \text{ or } \mathcal{H}_2}_{\text{Signal Present}} \text{ if} \\
& e^{-\frac{1}{2\sigma_n^2} \sum_{k=0}^{N-1} (\bar{r}[k] - \alpha_1 \bar{P}[k])^2} (1 - \hat{q}) + e^{-\frac{1}{2\sigma_n^2} \sum_{k=0}^{N-1} (\bar{r}[k] - \alpha_2 \bar{P}[k])^2} \hat{q} \\
& > e^{-\frac{1}{2\sigma_n^2} \sum_{k=0}^{N-1} \bar{r}[k]^2} \frac{\pi_0}{1 - \pi_0} \\
& \exp \left[-\frac{1}{2\sigma_n^2} \left(\alpha_1^2 \sum_{k=0}^{N-1} \bar{P}[k]^2 - 2\alpha_1 \sum_{k=0}^{N-1} \bar{r}[k] \bar{P}[k] \right) \right] (1 - \hat{q}) + \dots \\
& \exp \left[-\frac{1}{2\sigma_n^2} \left(\alpha_2^2 \sum_{k=0}^{N-1} \bar{P}[k]^2 - 2\alpha_2 \sum_{k=0}^{N-1} \bar{r}[k] \bar{P}[k] \right) \right] \hat{q} > \underbrace{\frac{\pi_0}{1 - \pi_0}}_{\eta}
\end{aligned} \tag{3.4}$$

The Bayes risk and composite hypothesis testing approaches in [1] both led to the decision rule shown in (3.4). The decision rule is constructed with only one potential unknown; namely, the prior probability of no-signal, π_0 . The availability of this value, as stated earlier, determines whether a CFAR or $\min(P_e)$ detection paradigm is employed. It can be seen that \hat{q} serves as a weight parameter here, representing the relative significance of the NLOS and LOS terms.

This generalized decision rule yields $\min(P_e)$ performance for an ensemble of trials when the true probability of LOS matches \hat{q} . This means that this decision rule can serve as a general rule encompassing all the knowledge cases that we discuss. The only differentiating factor is the estimated probability of LOS, \hat{q} , which can evolve with time in the most general case. Whereas, in [1], \hat{q} was either dynamic and binary or static and continuous, this work

introduces cases where the receiver's estimate of the probability of LOS evolves with time while taking on values anywhere between 0 and 1.

The performance analysis for this generalized decision rule requires the use of an approximation when deriving analytical expressions for the probability of detection (P_D) and false alarm (P_{FA}). This is necessary as there is no closed-form probability density function (PDF) for a Gaussian random variable (GRV) transformed by a weighted sum of exponential functions as is the case for (3.4). In [1], a piecewise-linear approximation was presented which considers the contribution of only one exponential term at a time, therefore making the logarithmic relationship between the matched-filter output, $\zeta(\vec{r})$, and the decision statistic a linear one. This then allows for the use of the standard Gaussian cumulative distribution function (CDF), $Q(\cdot)$ as it appears in the performance of the Neyman Pearson detector. In this chapter we expand the analysis of this piecewise approximation and show that it provides upper and lower bounds on detection performance.

$$\begin{aligned}
 T(\vec{r}) &= c_1 \exp(\Phi_1 \zeta(\vec{r})) + c_2 \exp(\Phi_2 \zeta(\vec{r})), \text{ where} \\
 c_1 &= (1 - \hat{q}) \exp\left(-\frac{\alpha_1^2 \epsilon(P)}{2\sigma_n^2}\right), \quad c_2 = \hat{q} \exp\left(-\frac{\alpha_2^2 \epsilon(P)}{2\sigma_n^2}\right), \\
 \Phi_1 &= \frac{\alpha_1}{\sigma_n}, \quad \Phi_2 = \frac{\alpha_2}{\sigma_n}, \quad \epsilon(P) = \sum_{k=0}^{N-1} \vec{P}[k]^2, \quad \zeta(\vec{r}) = \sum_{k=0}^{N-1} \vec{r}[k] \vec{P}[k]
 \end{aligned} \tag{3.5}$$

The piecewise approximation considers only the contribution from the most significant term of the decision statistic. The two regions are separated by a boundary point B which is defined as the point where the contribution of the NLOS and LOS terms to the overall decision statistic is the same. The decision statistic $T(\vec{r})$ can be written in a cleaner form by establishing the intermediate quantities shown in (3.5). As the NLOS and LOS exponential terms have different coefficients determined by the different signal amplitudes α_1 and α_2 , the contribution of one will rapidly eclipse the contribution of the other on either side of the

boundary B .

$$\log(T(\vec{r})) \approx \begin{cases} \log(c_1) + \Phi_1 \zeta(\vec{r}) & \zeta(\vec{r}) \leq B \\ \log(c_2) + \Phi_2 \zeta(\vec{r}) & \zeta(\vec{r}) > B \end{cases}$$

$$B = \frac{\log(\frac{c_2}{c_1})}{\Phi_1 - \Phi_2} = \log\left(\frac{\hat{q}}{1 - \hat{q}}\right) \frac{\sigma_n^2}{\alpha_1 - \alpha_2} + \frac{\epsilon(P)}{2} \left(\frac{\alpha_1^2 - \alpha_2^2}{\alpha_1 - \alpha_2}\right) \quad (3.6)$$

where B satisfies $c_1 e^{\Phi_1 B} = c_2 e^{\Phi_2 B}$.

$$\eta_1 = \frac{\sigma_n^2}{\alpha_1} \log\left(\frac{\pi_0}{(1 - \pi_0)(1 - \hat{q})}\right) + \frac{\alpha_1 \epsilon(P)}{2}$$

$$\eta_2 = \frac{\sigma_n^2}{\alpha_2} \log\left(\frac{\pi_0}{(1 - \pi_0)\hat{q}}\right) + \frac{\alpha_2 \epsilon(P)}{2}$$

The behavior of the weighted sum of exponential functions means that, when the matched filter output $\zeta(\vec{r})$ is significantly smaller or larger than B , the piecewise approximation is very accurate. On the other hand, when $\zeta(\vec{r}) \approx B$, the approximation drifts from the true decision statistic. In addition to being an approximation, the piecewise linear function is, in fact, a lower bound on detection performance. Furthermore, we can establish another piecewise linear function which serves as an upper bound.

As shown in [1], the piecewise approximation considers the most dominant term in the likelihood function to be the only term which allows one to analyze performance using a standard Neyman Pearson test. In this way, the threshold chosen is dependent upon which side of the boundary B the matched filter output $\zeta(\vec{r})$ falls. This produces two thresholds, η_1 for NLOS and η_2 for LOS, both presented in [1] and shown in (3.6). Due to the discarding of mutual contributions from NLOS and LOS states in the approximation, the ratio between the two amplitude values, α_1 and α_2 , has a direct effect on the exactness of the approximation. We can form the piecewise linear lower bound T_{lb} using the linear asymptotes of the decision statistic shown in (3.6). T_{lb} is asymptotically correct through this formulation, and the largest deviation from the optimal decision statistic occurs right at the boundary B . We

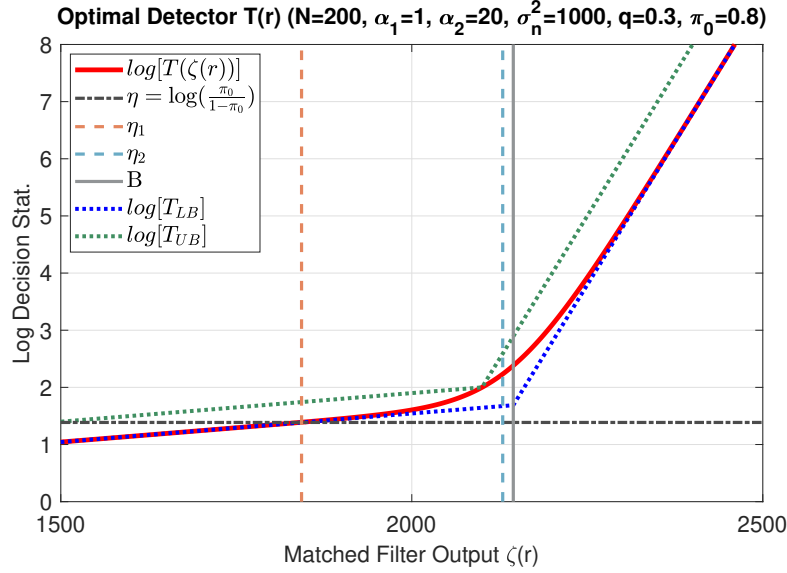


Figure 3.2: Optimal decision statistic with upper and lower bounds

can also establish that T_{LB} is a lower bound on the probability of detection P_D . As P_D is defined as $P_D = Pr[\{T(\zeta(\vec{r})) > \eta\} | \{\text{Signal Present}\}]$, and $T_{lb}(\zeta(\vec{r})) < T(\zeta(\vec{r})) \forall \zeta(\vec{r}) \in \mathbb{R}$, it follows that $P_{D-exact} > P_{D-LB}$. This same reasoning can be applied to the probability of false alarm P_{FA} as well.

$$\log(T_{LB}(\vec{r})) = \begin{cases} \log(c_1) + \Phi_1 \zeta(\vec{r}) & \zeta(\vec{r}) \leq B \\ \log(c_2) + \Phi_2 \zeta(\vec{r}) & \zeta(\vec{r}) > B \end{cases} \quad (3.7)$$

$$\log(T_{UB}(\vec{r})) = \begin{cases} -\frac{\alpha_1^2 \epsilon(P)}{2\sigma_n^2} + \Phi_1 \zeta(\vec{r}) & \zeta(\vec{r}) \leq \zeta\left(\frac{\alpha_1 + \alpha_2}{2}\right) \\ -\frac{\alpha_2^2 \epsilon(P)}{2\sigma_n^2} + \Phi_2 \zeta(\vec{r}) & \zeta(\vec{r}) > \zeta\left(\frac{\alpha_1 + \alpha_2}{2}\right) \end{cases}$$

Although the lower bound is accurate when the signal amplitude ratio $\frac{\alpha_2}{\alpha_1}$ is large, a small ratio is better represented by an upper bound. In the extreme case where $\alpha_2 = \alpha_1$, the optimal decision statistic collapses into a single term: $T(\zeta(\vec{r})) = \exp\left(-\frac{\alpha_1^2 \epsilon(P)}{2\sigma_n^2} + \frac{\alpha_1 \zeta(\vec{r})}{\sigma_n^2}\right)$. $T_{UB} = T$ in this extreme case and, for all other cases, it is defined as a piecewise linear function with a boundary located at the matched filter output of the average amplitude

value: $\zeta(\frac{\alpha_1 + \alpha_2}{2})$. As $T(\zeta(\vec{r}))$ is one-to-one, the same argument regarding P_D and P_{FA} for the lower bound can be made again here for the upper bound; namely, $P_{D-LB} < P_D \leq P_{D-UB}$ and $P_{FA-LB} < P_{FA} \leq P_{FA-UB}$.

The upper and lower bounds for the decision statistic are shown against the exact form in Figure 3.2 and defined explicitly in (3.7). One can see how the boundary B defines the point where the dominant contribution switches from the NLOS signal components to the LOS signal components. This makes intuitive sense because the detector should be more sensitive at lower matched filter outputs, reflecting the propensity for lower outputs to occur during NLOS periods.

3.3.1 Generalized Detection Performance

The detection performance of the generalized decision rule was analyzed in detail in [1]. The two paradigms of interest, as discussed earlier, are that of CFAR and $\min(P_e)$. Just as a generalized decision rule can be formed which encompasses all relevant types and degrees of LOS/NLOS knowledge available to the receiver, generalized probabilities of detections and false alarm (P_D and P_{FA}) can be formed as well.

In the most general form, P_D and P_{FA} are both functions of the independent parameter π_0 , the probability of the null / no-signal hypothesis. More specifically, π_0 appears as an argument of the threshold functions η_1 and η_2 spelled out in (3.6), and these thresholds are themselves arguments of the P_D and P_{FA} functions. Additionally, the true probability of LOS, q , is also an argument. The thresholds η_1 and η_2 along with the boundary B , which depend on the estimated probability of LOS, \hat{q} , are determined at the receiver, whereas q is a channel parameter not necessarily known at the receiver. In this way, they can be described

in the following form:

$$\begin{aligned} P_D &= f(\eta_1(\pi_0, \hat{q}), \eta_2(\pi_0, \hat{q}), B(\hat{q}), q) \\ P_{FA} &= g(\eta_2(\pi_0, \hat{q}), \eta_2(\pi_0, \hat{q}), B(\hat{q}), q) \end{aligned} \quad (3.8)$$

The general expressions for P_{D-LB} and P_{FA-LB} derived using the piecewise approximation are shown in (3.9). The expressions accommodate differing knowledge at the receiver depending on the true channel state which is important for cases with time-dependent, labeled knowledge. Additionally, the piecewise nature of P_{D-LB} and P_{FA-LB} stems from the piecewise nature of the decision rule in (3.4) where the boundary B marks the switch between NLOS dominance and LOS dominance. Here B , rather than being compared to the matched filter output $\zeta(\vec{r})$ as with the detector, is compared to η_1 . This is because $\eta_1 = \eta_2 = B$ marks the corresponding value of π_0 where the detector switches from using the NLOS threshold

η_1 to the LOS threshold η_2 .

$$\begin{aligned}
P_{D-LB} &= Pr [\text{Choose signal-present } |\mathcal{H}_1] = \\
&\underbrace{(1-q) [Pr [\zeta(\vec{r}) > \eta_1 | A_s = \alpha_1] 1 \{\eta_1 \leq B\}] + \dots}_{\text{NLOS channel, below boundary}} \\
&\underbrace{Pr [\zeta(\vec{r}) > \eta_2 | A_s = \alpha_1] 1 \{\eta_1 > B\}}_{\text{NLOS channel, above boundary}} + \dots \\
&\underbrace{q [Pr [\zeta(\vec{r}) > \eta_1 | A_s = \alpha_2] 1 \{\eta_1 \leq B\}] + \dots}_{\text{LOS channel, below boundary}} \\
&\underbrace{Pr [\zeta(\vec{r}) > \eta_2 | A_s = \alpha_2] 1 \{\eta_1 > B\}}_{\text{LOS channel, above boundary}} \\
\rightarrow P_{D-LB}(\eta_1(\pi_0, \hat{q}), \eta_2(\pi_0, \hat{q}), B(\hat{q}), q) &= \tag{3.9} \\
(1-q) Q \left(\underbrace{\frac{\eta_i(\hat{q}) - \alpha_1 \epsilon(P)}{\sigma_n \sqrt{\epsilon(P)}}}_{\hat{q}=\hat{q}_{NLOS}} \right) + q Q \left(\underbrace{\frac{\eta_i(\hat{q}) - \alpha_2 \epsilon(P)}{\sigma_n \sqrt{\epsilon(P)}}}_{\hat{q}=\hat{q}_{LOS}} \right) \\
\rightarrow P_{FA-LB}(\eta_1(\pi_0, \hat{q}), \eta_2(\pi_0, \hat{q}), B(\hat{q}), q) &= \\
(1-q) Q \left(\underbrace{\frac{\eta_i(\hat{q})}{\sigma_n \sqrt{\epsilon(P)}}}_{\hat{q}=\hat{q}_{NLOS}} \right) + q Q \left(\underbrace{\frac{\eta_i(\hat{q})}{\sigma_n \sqrt{\epsilon(P)}}}_{\hat{q}=\hat{q}_{LOS}} \right) \\
\text{where } i = \begin{cases} 1 & \eta_1(\hat{q}) \leq B(\hat{q}) \\ 2 & \eta_1(\hat{q}) > B(\hat{q}) \end{cases}
\end{aligned}$$

[1] details the special cases of *vision*, *statistical*, and *blind* knowledge and shows the resulting forms for P_D and P_{FA} in each case. It is found that in the *vision* case where $\hat{q} \in \{0, 1\}$, the performance can be simplified to the form in (3.10) where the boundary disappears and the performance expression becomes exact and no longer approximate. The binary nature of \hat{q} eliminates the need for mutual contributions between the NLOS and LOS terms in the

decision rule.

$$\begin{aligned}
 P_{D-V} &= \\
 & Q \left(\frac{\eta_1 - \alpha_1 \epsilon(P)}{\sigma_n \sqrt{\epsilon(P)}} \right) \Big|_{\hat{q}=0} (1 - q) + Q \left(\frac{\eta_2 - \alpha_2 \epsilon(P)}{\sigma_n \sqrt{\epsilon(P)}} \right) \Big|_{\hat{q}=1} q \\
 P_{FA-V} &= Q \left(\frac{\eta_1(\hat{q} = 0)}{\sigma_n \sqrt{\epsilon(P)}} \right) (1 - q) + Q \left(\frac{\eta_2(\hat{q} = 1)}{\sigma_n \sqrt{\epsilon(P)}} \right) q
 \end{aligned} \tag{3.10}$$

As the *vision* case involves dynamic detection instead of static detection for the *statistical* and *blind* cases, its performance depends simultaneously on both thresholds η_1 and η_2 . In the static detection cases, however, there is only a dependence upon one threshold at a time, and \hat{q} never changes. In [1] the claim is made that the CFAR performance of static detectors with unlabeled knowledge can never improve upon the uniformly most powerful (UMP) test which can be achieved with the use of a traditional Neyman Pearson detector. Here we will validate this claim.

As shown in (3.8), P_D and P_{FA} are most generally functions of both thresholds. In the absence of labeled information, however, a static detector will yield forms which are functions of just one threshold per piecewise component as shown in (3.11). This is important because the UMP test performance takes on the same functional form but with a single threshold η defined in 2.11.

$$\begin{aligned}
 P_{D-static}(\pi_0) &= f(\eta_k(\pi_0)); P_{FA-static}(\pi_0) = g(\eta_k(\pi_0)) \\
 & \text{where } k = 1 \{ \eta_1(\pi_0) > B \}
 \end{aligned} \tag{3.11}$$

$$P_{D-UMP} = f(\eta(\pi_0)); P_{FA-UMP} = g(\eta(\pi_0))$$

When analyzing CFAR performance, it is the implicit relationship between P_D and P_{FA} that matters because the operating point is determined by a pre-set P_{FA} value, not by any prior

knowledge of π_0 . We can show that the implicit function defined by $P_D(\pi_0)$ and $P_{FA}(\pi_0)$, otherwise known as the receiver operating characteristic (ROC) curve, is invariant to changes in the threshold function, $\eta_k(\pi_0)$ [34].

$$\text{Given that } f(\cdot) \text{ is one-to-one, } (f^{-1})'(x) = \frac{1}{f'(f^{-1}(x))}.$$

$$\text{Given } P_D(\pi_0) = f(\eta_k(\pi_0)) \text{ and } P_{FA}(\pi_0) = g(\eta_k(\pi_0)),$$

$$\frac{dp_d}{d\pi_0} = f'(\eta_k(\pi_0))\eta'_k(\pi_0) \text{ and } \frac{dp_{fa}}{d\pi_0} = g'(\eta_k(\pi_0))\eta'_k(\pi_0).$$

$$\begin{aligned} \text{Applying line 1, } \frac{d\pi_0}{dp_d} &= \frac{1}{f'(\eta_k(\eta_k^{-1}(f^{-1}(p_d))))\eta'_k(\eta_k^{-1}(f^{-1}(p_d)))} \\ &= \frac{1}{f'(f^{-1}(p_d))\eta'_k(\eta_k^{-1}(f^{-1}(p_d)))} = (f^{-1})'(p_d)(\eta_k^{-1})'(f^{-1}(p_d)). \end{aligned} \quad (3.12)$$

Using the symmetry of P_D and P_{FA} ,

$$\begin{aligned} \frac{dp_{fa}}{dp_d} &= \frac{(f^{-1})'(p_d)(\eta_k^{-1})'(f^{-1}(p_d))}{(g^{-1})'(p_{fa})(\eta_k^{-1})'(g^{-1}(p_{fa}))} \\ &= \frac{(f^{-1})'(p_d)(\eta_k^{-1})'(\pi_0)}{(g^{-1})'(p_{fa})(\eta_k^{-1})'(\pi_0)} = \frac{(f^{-1})'(p_d)}{(g^{-1})'(p_{fa})}. \\ \therefore \frac{dp_{fa}}{dp_d} &\text{ does not depend on the function } \eta_k(\pi_0). \end{aligned}$$

The implicit ROC curve can be fully defined by its slope $\frac{dp_{fa}}{dp_d}$, which does not depend on the common parameter π_0 . In (3.12) it is shown, by the inverse function theorem, that this slope in fact does not depend upon the threshold function $\eta_k(\pi_0)$, provided that P_D and P_{FA} are one-to-one which is clear from their definitions. As a consequence, the static detection performance of the *statistical* and *blind* cases is identical to that of the UMP test. This rule breaks as soon as some time-dependent knowledge is introduced into the detection framework; i.e., in the *vision* case where \hat{q} follows the true channel state $\Psi(t)$ at all times. As we will show in the following section, even imperfect labeled knowledge will yield performance that differs from the UMP test; although, whether an improvement is made depends on the fidelity of the knowledge available.

When analyzing $\min(P_e)$ performance, one finds that there is a dependence on the degree of static knowledge available which was showcased in [1] with the *statistical* case improving over the *blind* case under this paradigm. Additionally, there is no notion of a UMP test here because, rather than using a constant false-alarm rate, a particular value of π_0 is chosen based on prior knowledge of the probability of signal presence. The expression used for the error probability is simply a weighting of type-I and type-II errors based on prior knowledge of π_0 : $P_e = (1 - \pi_0)(1 - P_D) + \pi_0 P_{FA}$. The availability of static knowledge can be helpful for this type of performance because, unlike in CFAR, the performance at a specific operating point π_0 matters.

3.4 Optimal Detection with Periodic Labels

Having established a generalized detection framework that can accommodate all types of labeled and unlabeled knowledge, we can now turn our attention to the behavior of a receiver operating in a CTMC channel with periodic labels. The CTMC model allows us to explore the impact of imperfect labeled information which might be sourced from a more realistic sensor. Due to power and computation constraints, information regarding the NLOS/LOS state of the channel will never be continuously available in real systems as it is portrayed in [1] with the *vision* case. Instead this information is likely to be only intermittently available, similar to pilots in traditional channel estimation.

In the scenario at hand we establish a channel state process governed by a CTMC, $\Psi(t)$ with rate parameters λ_0 and λ_1 governing the tendency to jump between NLOS and LOS states. On top of this we define a label process $L(k)$ where labels are spaced apart by intervals of τ_L time units and occur with a certain probability of error ϵ . This model establishes two knobs for controlling the fidelity of the labels; i.e., the frequency of their occurrence $\frac{1}{\tau_L}$ and their

accuracy ϵ . In this way, the *vision* case outlined in [1] is simply a special case of periodic labels where $\tau_L = 0$ and $\epsilon = 0$, and the *statistical* or *blind* case arises whenever $\epsilon = 0.5$ or $\tau_L \rightarrow \infty$, depending on whether the stationary properties λ_0 and λ_1 are available to the receiver. This section will demonstrate that performance with periodic labels approaches the simplistic cases already explored when these regimes are approached.

As discussed in the last section, the optimal decision rule sources its knowledge of the channel state from \hat{q} , a value representing the receiver's best estimate of the true probability of LOS q at any point in time given the knowledge available to it. Naturally, if the knowledge available is time dependent, the estimate will evolve with time as well making $\hat{q}(t)$ a function of time. Furthermore, in the case of continuously available information ($\tau_L = 0$), $\hat{q}(t)$ is always up-to-date while, with periodic intermittent labels, \hat{q} is reflective of somewhat "old" information.

$$\begin{cases} Pr [L(k) = \Psi(t_k)] = 1 - \epsilon \\ Pr [L(k) = 1 - \Psi(t_k)] = \epsilon \end{cases} \quad (3.13)$$

$$Pr [LOS | \{L(k) = \Lambda\}] = \frac{Pr[\{L(k) = \Lambda\} | LOS] Pr[LOS]}{Pr[L(k) = \Lambda]}$$

$$\hat{q}(t_k) = \begin{cases} L(k), & \epsilon \text{ unknown} \\ \epsilon(1 - L(k)) + (1 - \epsilon)L(k), & \epsilon \text{ known, } q \text{ unknown} \\ \frac{\epsilon q}{\epsilon q + (1 - \epsilon)(1 - q)}(1 - L(k)) + \dots \\ \frac{(1 - \epsilon)q}{(1 - \epsilon)q + \epsilon(1 - q)}L(k), & \epsilon, q \text{ known} \end{cases} \quad (3.14)$$

First, we will look at the behavior with imperfect, continuous vision. As the labels are continuously available, there is no need to consider the behavior in between labels. $\hat{q}(t)$ is therefore updated continuously based on the current label value. This behavior is then dependent upon whether the receiver knows the label error probability ϵ and whether it knows the true probability of LOS, q . Under imperfect labels, the PMF for the label process

is shown in (3.13). If the receiver doesn't know the error probability itself or cannot obtain a good estimate for it, the labels are simply blindly trusted, making $\hat{q}(t_k)$ simply equal to the current label value $L(k)$ as shown in (3.14). When ϵ is known, however, the receiver can use this knowledge to estimate the current probability of LOS either with or without knowledge of the stationary probability of LOS, q . With both ϵ and q known, an optimal estimate can be found through Bayes' Theorem which incorporates the stationary CTMC behavior into the estimate. In this formulation, $\hat{q}(t_k) = q$ when $\epsilon = 0.5$, reflecting the lack of information in the labels in this case. On the other hand, with $\epsilon = \{0, 1\}$, the estimate relies solely on the label value, not q .

To explore the receiver's behavior between the labels, we need to know the temporal properties of the CTMC process. As discussed in the system model, the CTMC is defined by its generator matrix, $Q_\Psi = \begin{bmatrix} -\lambda_0 & \lambda_0 \\ \lambda_1 & -\lambda_1 \end{bmatrix}$. The Markovian property of the process means that the probability of the channel state changing from some value at t_1 to some other value at t_2 is dependent only upon the time duration $t_2 - t_1$ [35]. The state probability for the CTMC in between labels can then be represented by the transient probability distribution for the CTMC.

The transient probability represents the expected state of the CTMC τ time units before or after a known state or known probability of a state. It is found using the matrix exponential of the generator matrix: $e^{Q_\Psi \tau}$. If $\{\bar{g}_1, \bar{g}_2\}$ are the right eigenvectors of Q_Ψ and $\{\bar{f}_1, \bar{f}_2\}$ are

the left eigenvectors, the matrix exponential is given by: $e^{Q_\Psi\tau} = e^{-(\lambda_0+\lambda_1)\tau}\bar{g}_1\bar{f}_1 + \bar{g}_2\bar{f}_2$. [35].

$$\begin{aligned}
e^{Q_\Psi\tau} &= \begin{bmatrix} \pi_{00}(\tau) & \pi_{01}(\tau) \\ \pi_{10}(\tau) & \pi_{11}(\tau) \end{bmatrix} = \\
&\begin{bmatrix} Pr[\{\Psi(\tau) = 0\} | \{\Psi(0) = 0\}] & Pr[\{\Psi(\tau) = 1\} | \{\Psi(0) = 0\}] \\ Pr[\{\Psi(\tau) = 0\} | \{\Psi(0) = 1\}] & Pr[\{\Psi(\tau) = 1\} | \{\Psi(0) = 1\}] \end{bmatrix} = \\
&\begin{bmatrix} e^{-(\lambda_0+\lambda_1)|\tau|}\frac{\lambda_0}{\lambda_0+\lambda_1} + \frac{\lambda_1}{\lambda_0+\lambda_1} & -e^{-(\lambda_0+\lambda_1)|\tau|}\frac{\lambda_0}{\lambda_0+\lambda_1} + \frac{\lambda_0}{\lambda_0+\lambda_1} \\ -e^{-(\lambda_0+\lambda_1)|\tau|}\frac{\lambda_1}{\lambda_0+\lambda_1} + \frac{\lambda_1}{\lambda_0+\lambda_1} & e^{-(\lambda_0+\lambda_1)|\tau|}\frac{\lambda_1}{\lambda_0+\lambda_1} + \frac{\lambda_0}{\lambda_0+\lambda_1} \end{bmatrix} \\
&= \begin{bmatrix} e^{-\lambda'|\tau|}q + (1-q) & -e^{-\lambda'|\tau|}q + q \\ -e^{-\lambda'|\tau|}(1-q) + (1-q) & e^{-\lambda'|\tau|}(1-q) + q \end{bmatrix} \tag{3.15}
\end{aligned}$$

Computing the matrix exponential yields the 2×2 result in (3.15). As described earlier, there is a clear dependence on the time duration τ , specifically that of exponential decay. This is consistent with the exponentially distributed holding times in the definition of the CTMC. It is also noteworthy that the rate of decay is the sum of the rate parameters which we denote $\lambda' = \lambda_0 + \lambda_1$. The transient probabilities also converge to the stationary distribution $\bar{\pi} = \begin{bmatrix} (1-q) & q \end{bmatrix}$ as $\tau \rightarrow \infty$ representing the lack of temporal correlation after a long enough duration. For ease of notation, the transient probabilities are represented by $\pi_{ij}(\tau)$ where i is the conditioned state and j is the outcome after τ time units. The transient probability's dependence only on the elapsed time points to the Markov nature of the process and samples of the process as well. This indicates that the label process is also Markov, meaning that a receiver with periodic labeled knowledge of the LOS state need only reference the most recent label, and no previous labels, to determine the best estimate for the probability of

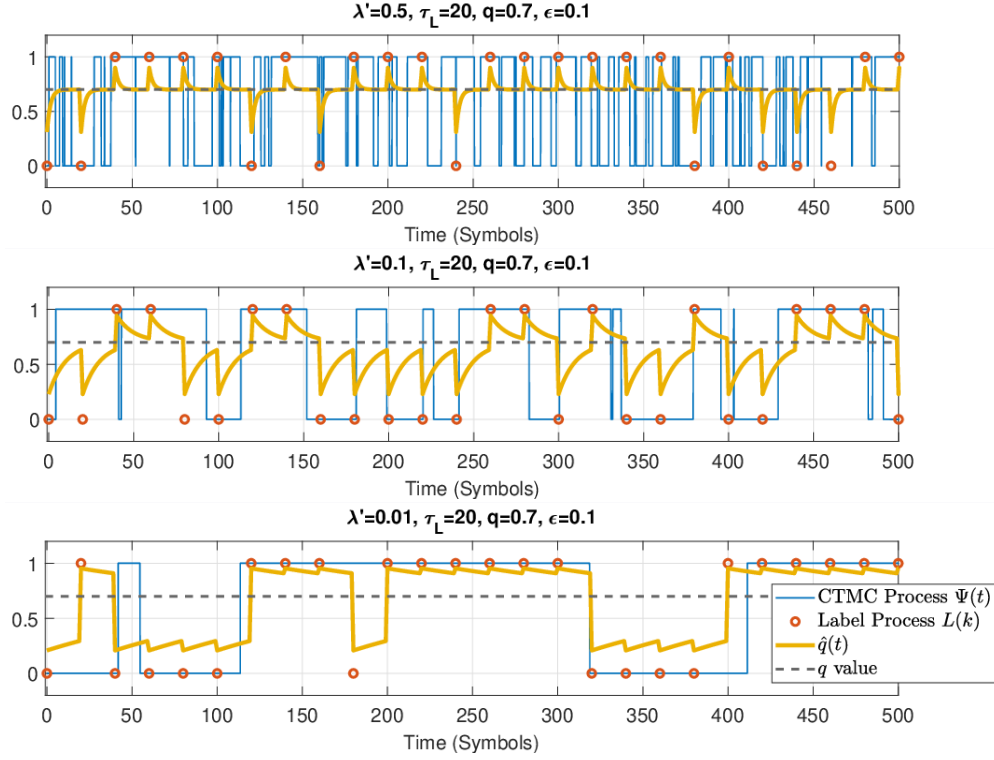


Figure 3.3: LOS prob. estimate $\hat{q}(t)$ at the receiver with CTMC channel state $\Psi(t)$ and CTMC rates of $\lambda' = \{0.5, 0.1, 0.01\}$

LOS at any point in time.

$$\begin{aligned}
 & Pr[\{\Psi(t_k + \tau) = 1\} | \{L(k) = \Lambda\}] = \\
 & Pr[\{\Psi(t_k + \tau) = 1\} | \{\Psi(t_k) = \Lambda\}]Pr[\text{Correct Label}] + \\
 & Pr[\{\Psi(t_k + \tau) = 1\} | \{\Psi(t_k) = 1 - \Lambda\}]Pr[\text{Errored Label}] \\
 \rightarrow \hat{q}_{PL}(t) = & \begin{cases} \pi_{01}(t - t_k) \left(\frac{(1-\epsilon)(1-q)}{(1-\epsilon)(1-q) + \epsilon q} \right) + \dots & L(k) = 0 \\ \pi_{11}(t - t_k) \left(\frac{\epsilon q}{(1-\epsilon)(1-q) + \epsilon q} \right), & L(k) = 0 \\ \pi_{11}(t - t_k) \left(\frac{(1-\epsilon)q}{(1-\epsilon)q + \epsilon(1-q)} \right) + \dots & L(k) = 1 \\ \pi_{01}(t - t_k) \left(\frac{\epsilon(1-q)}{(1-\epsilon)q + \epsilon(1-q)} \right), & L(k) = 1 \end{cases} \quad (3.16)
 \end{aligned}$$

where $t - t_k$ is the *label age*.

To obtain the final estimate for the probability of LOS, the receiver must factor in the label error rate ϵ , which can be done using the expressions shown in (3.14), and the *label age* which we define as the time elapsed since the most recent label, $t - t_k$. The final expression shown in (3.16) involves the transient probabilities π_{01} and π_{11} weighted by the probability of the channel state at the time of the most recent label, t_k , conditioned upon the label state. These expressions now form the receiver's best estimate for the average state of the CTMC channel at any time since the last known label $L(k)$ given that the stationary parameters λ_0 , λ_1 , and the label error rate ϵ are known at the receiver.

When adopting the $\hat{q}_{PL}(t)$ scheme in (3.16) with periodic labeled knowledge, the resulting behavior is depicted in Figure 3.3. Here, the value $\hat{q}_{PL}(t)$ is shown in three different scenarios with different CTMC rates: $\lambda' = \{0.5, 0.1, 0.05\}$. The label spacing is kept constant at $\tau_L = 20$ with a label error rate of $\epsilon = 0.1$. One can see how the $\hat{q}(t)$ value spikes towards the label value when each label is received, but decays towards the stationary probability of LOS, q , very rapidly with a fast CTMC. On the other hand, with a slower CTMC $\hat{q}(t)$ remains closer to the label value until the next label occurs. This indicates the convergence towards the *vision* case when the label spacing becomes small compared to the reciprocal of the CTMC rate, $\tau_L \ll 1/\lambda'$, and towards the *statistical* case when the opposite is true.

3.4.1 Performance Analysis with Periodic Labels

Having detailed the optimal LOS estimate based on periodic labeled knowledge, we can now delve into the detection performance of such a vision-enhanced receiver under both CFAR and $\min(P_e)$ paradigms. The generalized performance expressions presented in section 3.1 form a template through which we can derive the performance for periodic labeled knowledge. The approach here is to apply the $\hat{q}_{PL}(t)$ expressions to the generalized P_{D-LB} and P_{FA-LB}

to obtain the performance given the true channel state during the current symbol, $\Psi(0)$, the most recent label value seen by the receiver, $L(k)$, and the corresponding label age. The final performance can then be found by marginalizing over the distribution of true states and labeled state combinations as well as the distribution of label ages.

The general expressions for P_D and P_{FA} feature a single argument for \hat{q} , the estimated probability of LOS at the receiver. In the *statistical* case, only one version of this knowledge was required to represent the overall performance because the knowledge did not change based on the true conditions over time. In contrast, the *vision* case featured two types of knowledge: one with $\hat{q} = 0$ which occurred only during true NLOS periods and one with $\hat{q} = 1$ during true LOS periods. With periodic labels we have a more nuanced situation where the knowledge of the probability of LOS changes depending on the current true state at the time of the symbol of interest; however, there is some probability of receiving outdated information that is no longer accurate.

This degree of nuance means that we must consider when the labels match the true channel state at the symbol of interest and when they do not. Since the receiver's knowledge of the LOS state is ultimately coming from the labels, their accuracy determines the \hat{q} estimate used during NLOS and LOS periods. The final expressions for P_D and P_{FA} for periodic labels must therefore use the probability of matching and mismatching labels to weight the

outcomes.

$$\begin{aligned}
\hat{q}_{NLOS-PL}(t) &= \pi_{01}(t - t_k)\Omega_1 + \pi_{11}(t - t_k)(1 - \Omega_1) \\
\hat{q}_{LOS-PL}(t) &= \pi_{11}(t - t_k)\Omega_2 + \pi_{01}(t - t_k)(1 - \Omega_2) \\
\text{where } \Omega_1 &= \left(\frac{(1 - \epsilon)(1 - q)}{(1 - \epsilon)(1 - q) + \epsilon q} \right), \Omega_2 = \left(\frac{(1 - \epsilon)q}{(1 - \epsilon)q + \epsilon(1 - q)} \right) \\
P_{D-PL} &= \frac{1}{\tau_L} \int_{t=0}^{\tau_L} \underbrace{P_{D-LB}(\hat{q}_1)}_{\text{label matches } \Psi} c(t) + \underbrace{P_{D-LB}(\hat{q}_2)}_{\text{label does not match } \Psi} (1 - c(t)) dt \\
P_{FA-PL} &= \frac{1}{\tau_L} \int_{t=0}^{\tau_L} P_{FA-LB}(\hat{q}_1)c(t) + P_{FA-LB}(\hat{q}_2)(1 - c(t)) dt
\end{aligned} \tag{3.17}$$

where

$$\hat{q}_1 = \begin{cases} \hat{q}_{NLOS-PL}, & \Psi = 0 \\ \hat{q}_{LOS-PL}, & \Psi = 1 \end{cases}, \hat{q}_2 = \begin{cases} \hat{q}_{LOS-PL}, & \Psi = 0 \\ \hat{q}_{NLOS-PL}, & \Psi = 1 \end{cases},$$

$$c(t) = (1 - \epsilon) ((1 - q)\pi_{00}(t) + q\pi_{11}(t)) + \epsilon ((1 - q)\pi_{01}(t) + q\pi_{10}(t))$$

Merely weighting the outcomes based on the label accuracy does represent average performance, but only for one particular value of $t - t_k$, the label age. The overall ensemble performance must marginalize over the distribution of these ages. Since the label period τ_L is a stationary parameter; i.e., it is constant, the distribution of label ages is uniform over the label period. This reflects the fact that symbols are equally-likely to occur at any point between two consecutive labels. (3.17) shows the final detection and false-alarm probabilities for the periodic labels case taking all this into account. Cases involving matching and mismatching labels are weighted by $c(t)$, the probability that the label in question matches.

3.5 Numerical Results and Discussion

Having laid out a detection framework which encompasses all of the nuances introduced when vision information is discontinuous and prone to error, we can now explore the performance of a detector employing such a framework through both analytical and numerical comparisons in various performance paradigms. In the Chapter 2, performance under three basic knowledge cases, *vision*, *statistical*, and *blind*, was showcased under the CFAR and $\min(P_e)$ paradigms. Here we expand this into the more nuanced case of periodic labels where parameters such as the label period τ_L and the label error probability ϵ can control the fidelity of the information available at the receiver.

A CTMC channel simulation was constructed in which 100k symbols are detected using the optimal decision rule shown in (3.4). Four knowledge cases are simulated: 1) *Perfect Vision*, 2) *Periodic Labels*, 3) *Statistical*, and 4) *Blind* knowledge. For each knowledge case the corresponding estimate for the current probability of LOS ($\hat{q}(t)$) is applied for each symbol. $\hat{q}(t)$ is then applied to the detection decision and results are tabulated.

The first set of results pertains to the CFAR paradigm for which Figures 3.4, 3.5, and 3.6 are relevant. A comparison is made here between varying degrees of labeled knowledge at the receiver and the UMP test which serves as a baseline for CFAR performance. As discussed earlier, the performance with any kind of unlabeled knowledge will always match the UMP test under CFAR (see (3.11)). Figure 3.4 shows the receiver operating characteristic (ROC) performance under the aforementioned knowledge cases. The gains through the vision information appear for three different values for the true prob. of LOS ($q = \{0.2, 0.5, 0.8\}$); however, greater gains are achieved with higher q values. As expected, the performance with *periodic labels* falls in between *perfect vision* and the UMP test and is upper- and lower-bounded by the two.

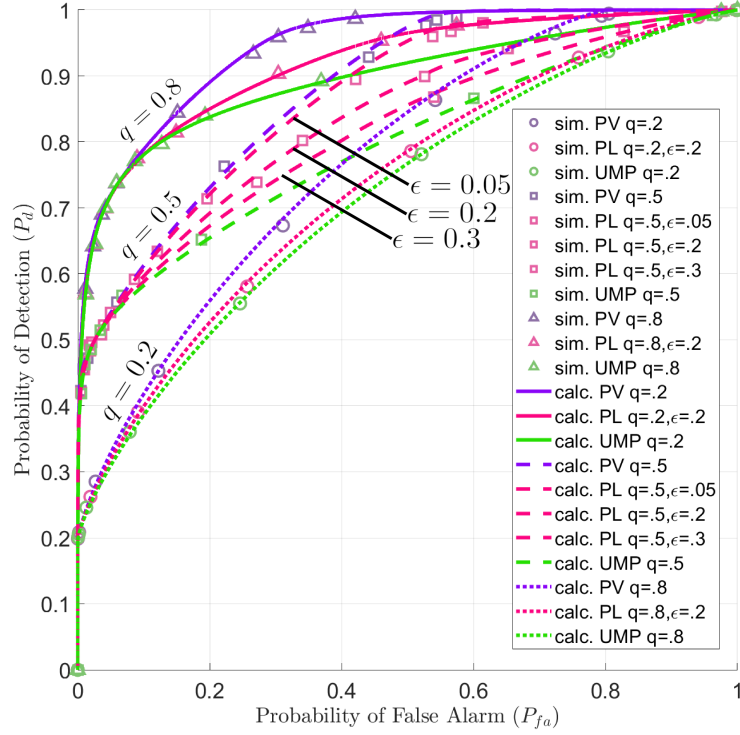


Figure 3.4: Simulated and calculated ROC curves for Perfect Vision (PV), Periodic Labels (PL), and UMP test with $\text{SNR}_{avg} = 8$ dB, $q = \{0.2, 0.5, 0.8\}$, $\alpha_2/\alpha_1 = 10$, $\lambda' = 0.1$, $\tau_L = 1$

Figure 3.5 provides a different angle for CFAR performance, showing probability of detection across average SNR values for a target false alarm rate of $P_{FA} = 0.1$. Note that the average SNR is calculated as $\text{SNR}_{avg} = \frac{\epsilon(P)((1-q)\alpha_1^2 + q\alpha_2^2)}{\sigma_n^2}$. Here, once again, a gradient in performance is observed from the UMP test with the lowest P_D across the board to *periodic labels* to *perfect vision*. Below $\text{SNR}_{avg} = 0$ dB, however, the simulated data diverges from the analytical results. This can be attributed to the use of the piecewise-linear lower bound in (3.7) for the optimal decision rule and in the receiver's calculation of the π_0 values used based upon the set P_{FA} value.

Figure 3.6 like Figure 3.5 shows the probability of detection under CFAR with $P_{FA} = 0.1$; however, instead of sweeping over SNR we sweep over the label period τ_L in units of

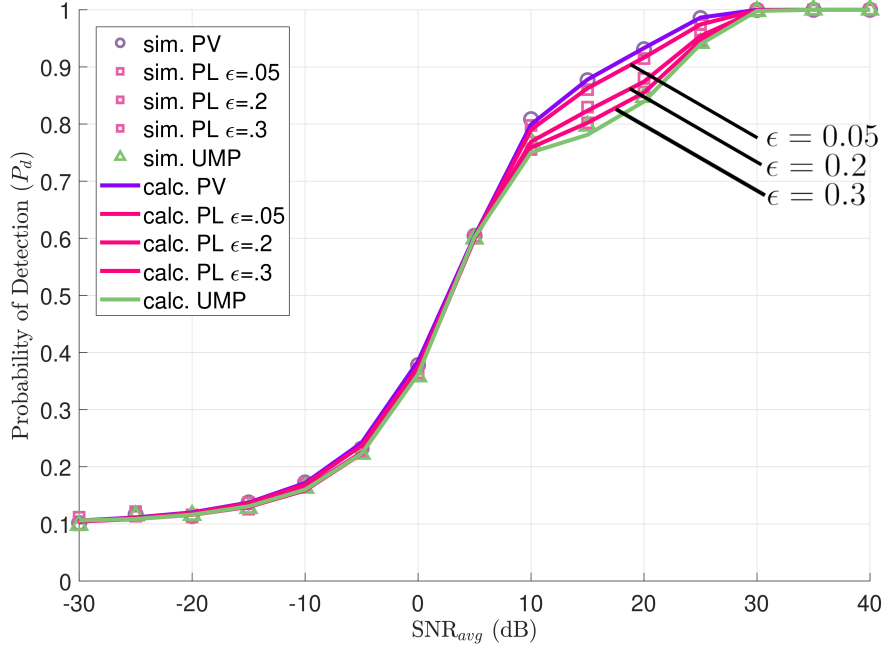


Figure 3.5: CFAR Prob. of Detection vs avg. SNR for Perfect Vision (PV), Periodic Labels (PL), and UMP test with Target $P_{FA} = 0.1$, $q = 0.7$, $\alpha_2/\alpha_1 = 10$, $\lambda' = 0.1$, $\tau_L = 1$

time. This result demonstrates the effect of the channel sample rate and label error rate on performance when compared to the two special cases of *perfect vision* and the UMP test. One can see how labels which occur more often achieve performance which approaches *perfect vision* while sparse labels approach the performance of the UMP test. Additionally, introducing label errors translates to a shift towards the UMP performance overall. This behavior is expected because the useful time-dependent information available from *periodic labels* decreases as the label rate ($1/\tau_L$) becomes much smaller than the CTMC rate (λ').

Performance under the $\min(P_e)$ paradigm for all knowledge cases is presented in Figure 3.7. Here the overall error rate is measured wherein $P_e = (1 - P_D)(1 - \pi_0) + P_{FA}\pi_0$ and equal weight is placed on false alarms and missed detections with $\pi_0 = 0.5$. One can observe how the bimodal nature of the likelihood function manifests with two separate dips in the error rate occurring approximately 40 dB apart. This is consistent with the chosen amplitude

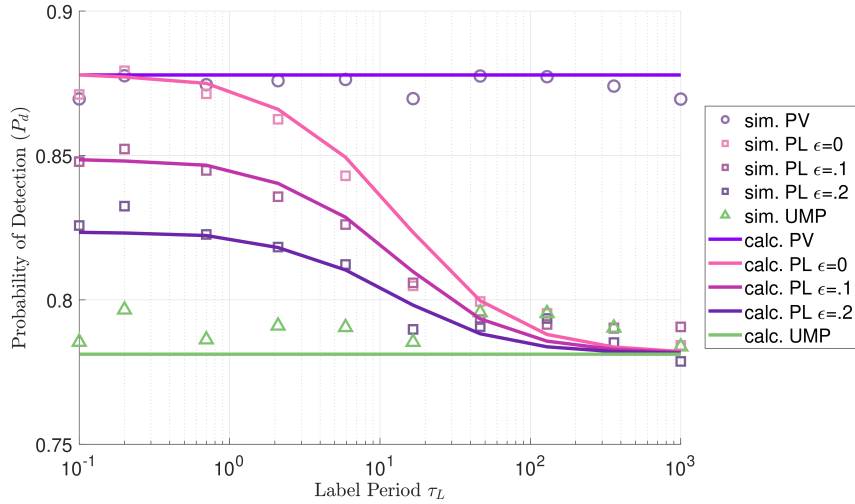


Figure 3.6: CFAR Prob. of Detection vs label period (τ_L) for Perfect Vision (PV), Periodic Labels (PL), and UMP test with Target $P_{FA} = 0.1$, $q = 0.7$, $\alpha_2/\alpha_1 = 10$, $\lambda' = 0.1$, $\epsilon = \{0, 0.1, 0.2\}$

ratio of $\alpha_2/\alpha_1 = 100$. Here a gradient in performance is observed once again, but crucially the *statistical* case now out-performs the *blind* case unlike the UMP-test equivalence seen in the CFAR paradigm. It should also be noted that the UMP test is irrelevant for $\min(P_e)$ performance. Additionally, the gain is achieved within a particular SNR range with the *perfect vision* case yielding an approximate 10 dB improvement at $P_e = 4 \cdot 10^{-2}$. This localized gain is consistent with the fact that, at lower SNR values, intermittent LOS conditions provide little benefit while, at higher SNR values, intermittent NLOS conditions provide little hindrance.

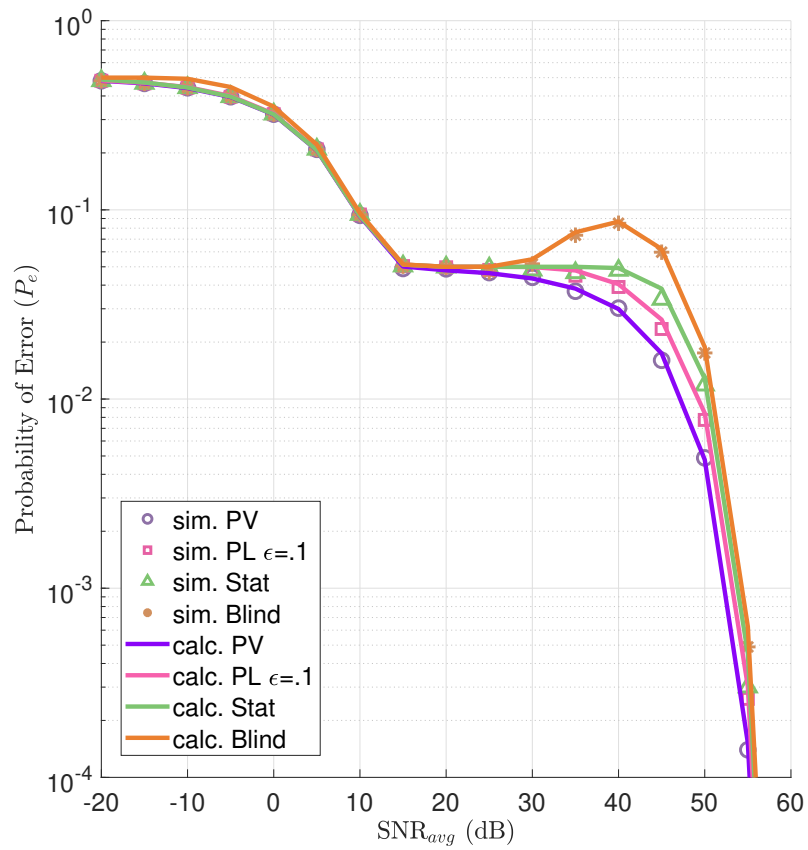


Figure 3.7: Probability of Error vs avg. SNR for Perfect Vision (PV), Periodic Labels (PL), Statistical (S), and Blind (B) with $q = 0.9$, $\alpha_2/\alpha_1 = 100$, $\lambda' = 0.1$, $\epsilon = 0.1$, $\tau_L = 1$

Chapter 4

Conclusion

The exploration we have undertaken here demonstrates the value of external *vision* information in wireless communications systems under intermittent NLOS/LOS conditions. By introducing labeled knowledge of the LOS state one can achieve a higher probability of detection for any given probability of false alarm in an ensemble of trials. Furthermore, unlabeled statistical information about the LOS state cannot improve upon the UMP test under a CFAR paradigm; although, when the prior probability of the null hypothesis, π_0 , is known at the receiver, unlabeled statistical information can yield a lower overall error rate.

The benefits achieved with vision sensors are most pronounced under conditions in which the NLOS/LOS state has a severe impact on received signal strength. This is reflected in the construction of the optimal decision statistic wherein the relative impact of the NLOS and LOS terms is determined in part by the ratio between amplitude values α_2/α_1 .

Scenarios in which labeled information is not continuously available are also shown to improve CFAR detection performance over the UMP test. The CTMC channel model presented provides generalized framework which can be catered towards a variety of realistic propagation scenarios. Cameras which capture optical data at rates comparable to or slower than the NLOS/LOS toggling rate can be represented as sparse labels, for instance. Even when the label rate ($1/\tau_L$) becomes much smaller than the CTMC rate λ_1 , performance gains over the UMP test are still observed.

As the interconnected world becomes more dominated by automation and machine-to-machine communication, the integration of sensors with existing physical layer systems is becoming more and more valuable. This work demonstrates how these sensors can help on the most fundamental level, and expansion of this work towards other forms of vision information, such as other forms of direct geometric sensing as discussed in Chapter 1, can be done using the same hypothesis testing techniques presented here.

The composite hypothesis testing framework presented here involves a single unknown parameter, the received signal amplitude A_s . The process used here to incorporate vision information into the optimal decision rule can be applied to any form of direct geometric sensing simply by introducing different or additional unknown parameters and their associated distributions for each knowledge case. An analysis of angle-of-arrival based vision, for instance, could utilize a MIMO version of the detection framework presented wherein the array factor has some known distribution based upon the knowledge of the angle-of-arrival. The subsequent steps involving the optimal decision rule and performance derivations would follow the same general procedure.

Bibliography

- [1] S. B. Brown and H. S. Dhillon, “Improving receiver detection performance through NLOS/LOS vision,” in *MILCOM 2024 - 2024 IEEE Military Communications Conference (MILCOM)*, 2024, pp. 1–6.
- [2] F. Duarte, “60+ amazing IoT statistics (2024-2030),” Sep 2024. [Online]. Available: <https://explodingtopics.com/blog/iot-stats>
- [3] L. Dignan, “IoT devices to generate 79.4zb of data in 2025, says IDC,” Jun 2019. [Online]. Available: <https://www.zdnet.com/article/iot-devices-to-generate-79-4zb-of-data-in-2025-says-idc/>
- [4] H. S. Dhillon, H. Huang, and H. Viswanathan, “Wide-area wireless communication challenges for the internet of things,” *IEEE Communications Magazine*, vol. 55, no. 2, pp. 168–174, 2017.
- [5] F. Liu, Y. Cui, C. Masouros, J. Xu, T. X. Han, Y. C. Eldar, and S. Buzzi, “Integrated sensing and communications: Toward dual-functional wireless networks for 6g and beyond,” *IEEE Journal on Selected Areas in Communications*, vol. 40, no. 6, pp. 1728–1767, 2022.
- [6] N. González-Prelcic, M. Furkan Keskin, O. Kaltiokallio, M. Valkama, D. Dardari, X. Shen, Y. Shen, M. Bayraktar, and H. Wymeersch, “The integrated sensing and communication revolution for 6g: Vision, techniques, and applications,” *Proceedings of the IEEE*, vol. 112, no. 7, pp. 676–723, 2024.
- [7] J. A. Zhang, A. Cantoni, X. Huang, Y. J. Guo, and R. W. Heath, “Framework for an

- innovative perceptive mobile network using joint communication and sensing,” in *2017 IEEE 85th Vehicular Technology Conference (VTC Spring)*, 2017, pp. 1–5.
- [8] A. Zhang, M. L. Rahman, X. Huang, Y. J. Guo, S. Chen, and R. W. Heath, “Perceptive mobile networks: Cellular networks with radio vision via joint communication and radar sensing,” *IEEE Vehicular Technology Magazine*, vol. 16, no. 2, pp. 20–30, 2021.
- [9] X. Tu, H. Li, and H. S. Dhillon, “Information-theoretic analysis of vision-aided isac over a discrete memoryless channel,” in *2024 IEEE 100th Vehicular Technology Conference (VTC2024-Fall)*, 2024, pp. 1–7.
- [10] X. Cheng, Y. Li, C.-X. Wang, X. Yin, and D. W. Matolak, “A 3-d geometry-based stochastic model for unmanned aerial vehicle mimo rician fading channels,” *IEEE Internet of Things Journal*, vol. 7, no. 9, pp. 8674–8687, 2020.
- [11] L. Azpilicueta, A. Schultze, M. Celaya-Echarri, F. A. Rodríguez-Corbo, C. Constantinou, R. M. Shubair, F. Falcone, and M. Navarro-Cía, “Diffuse-scattering-informed geometric channel modeling for thz wireless communications systems,” *IEEE Transactions on Antennas and Propagation*, vol. 71, no. 10, pp. 8226–8238, 2023.
- [12] A. Ali, N. González-Prelcic, and R. W. Heath, “Spatial covariance estimation for millimeter wave hybrid systems using out-of-band information,” *IEEE Transactions on Wireless Communications*, vol. 18, no. 12, pp. 5471–5485, 2019.
- [13] Z. Li, C. Zhang, I.-T. Lu, and X. Jia, “Hybrid precoding using out-of-band spatial information for multi-user multi-rf-chain millimeter wave systems,” *IEEE Access*, vol. 8, pp. 50 872–50 883, 2020.
- [14] S. M. Kay, *Fundamentals of Statistical Signal Processing: Detection Theory*. Prentice-Hall PTR, 1998.

- [15] A. Ghobadzadeh, S. Gazor, M. Naderpour, and A. A. Tadaion, “Asymptotically optimal CFAR detectors,” *IEEE Trans. on Signal Processing*, vol. 64, no. 4, pp. 897–909, 2016.
- [16] M. Naderpour, A. Ghobadzadeh, A. Tadaion, and S. Gazor, “Generalized wald test for binary composite hypothesis test,” *IEEE Signal Processing Letters*, vol. 22, no. 12, pp. 2239–2243, 2015.
- [17] O. Harel and H. Messer, “Extension of the MFLRT to detect an unknown deterministic signal using multiple sensors, applied for precipitation detection,” *IEEE Signal Processing Letters*, vol. 20, no. 10, pp. 945–948, 2013.
- [18] S. Bar and J. Tabrikian, “Adaptive waveform design for target detection with sequential composite hypothesis testing,” in *2016 IEEE Statistical Signal Processing Workshop (SSP)*, 2016, pp. 1–5.
- [19] —, “A sequential framework for composite hypothesis testing,” *IEEE Transactions on Signal Processing*, vol. 66, no. 20, pp. 5484–5499, 2018.
- [20] S. Bayram and S. Gezici, “On the restricted neyman–pearson approach for composite hypothesis-testing in presence of prior distribution uncertainty,” *IEEE Transactions on Signal Processing*, vol. 59, no. 10, pp. 5056–5065, 2011.
- [21] J. Liu, Y. Ma, J. Wang, N. Yi, R. Tafazolli, S. Xue, and F. Wang, “A non-stationary channel model with correlated NLOS/LOS states for elaa-mmimo,” in *2021 IEEE Global Communications Conference (GLOBECOM)*, 2021, pp. 1–6.
- [22] L. Yi, S. G. Razul, Z. Lin, and C.-M. See, “Individual aoameasurement detection algorithm for target tracking in mixed LOS/NLOS environments,” in *2013 IEEE International Conference on Acoustics, Speech and Signal Processing*, 2013, pp. 3924–3928.
- [23] E. L. Lehmann, *Testing Statistical Hypotheses*. Springer, 2005.

- [24] L. Chettri and R. Bera, “A comprehensive survey on internet of things (IoT) toward 5g wireless systems,” *IEEE Internet of Things Journal*, vol. 7, no. 1, pp. 16–32, 2020.
- [25] G. Colistra and L. Atzori, “Estimation of physical layer performance in wsns exploiting the method of indirect observations,” *Journal of Sensor and Actuator Networks*, vol. 1, no. 3, pp. 272–298, 2012. [Online]. Available: <https://www.mdpi.com/2224-2708/1/3/272>
- [26] F. Guo, F. R. Yu, H. Zhang, X. Li, H. Ji, and V. C. M. Leung, “Enabling massive IoT toward 6g: A comprehensive survey,” *IEEE Internet of Things Journal*, vol. 8, no. 15, pp. 11 891–11 915, 2021.
- [27] A. Ali, N. González-Prelcic, and R. W. Heath, “Millimeter wave beam-selection using out-of-band spatial information,” *IEEE Transactions on Wireless Communications*, vol. 17, no. 2, pp. 1038–1052, 2018.
- [28] T. Ma, Y. Xiao, X. Lei, and M. D. Renzo, “Integrated sensing and communication with reconfigurable intelligent surfaces,” *IEEE Transactions on Vehicular Technology*, vol. 73, no. 12, pp. 19 051–19 064, 2024.
- [29] S. Kim, Y. Ahn, D. Park, and B. Shim, “Vomtc: Vision objects for millimeter and terahertz communications,” *IEEE Transactions on Cognitive Communications and Networking*, vol. 11, no. 1, pp. 243–257, 2025.
- [30] Z. Ying, H. Yang, J. Gao, and K. Zheng, “A new vision-aided beam prediction scheme for mmwave wireless communications,” in *2020 IEEE 6th International Conference on Computer and Communications (ICCC)*, 2020, pp. 232–237.
- [31] M. Mushkin and I. Bar-David, “Capacity and coding for the gilbert-elliott channels,” *IEEE Transactions on Information Theory*, vol. 35, no. 6, pp. 1277–1290, 1989.

- [32] H. Kong and E. Shwedyk, “Sequence detection and channel state estimation over finite state markov channels,” *IEEE Transactions on Vehicular Technology*, vol. 48, no. 3, pp. 833–839, 1999.
- [33] W. J. Anderson, *Differentiability Properties of Transition Functions and the Significance of the Q-Matrix*. Springer-Verlag, 1991, p. 8–21.
- [34] A. Weinstein and J. E. Marsden, *Inverse Functions and the Chain Rule*. Benjamin/Cummings Pub. Co., 1980, p. 100–113.
- [35] G. R. Murthy and D. G. Down, “Autocorrelation function characterization of continuous time markov chains,” 2019. [Online]. Available: <https://arxiv.org/abs/1908.09284>